Contrib Mineral Petrol (1999) 135: 255–276

Antonio Castro · Alberto E. Patiño Douce · L. Guillermo Corretgé · Jesús D. de la Rosa · Mohammed El-Biad · Hassan El-Hmidi

Origin of peraluminous granites and granodiorites, Iberian massif, Spain: an experimental test of granite petrogenesis

Received: 30 June 1998 / Accepted: 27 November 1998

Abstract The discrimination between potential source materials involved in the genesis of Iberian granites and granodiorites, as well as the role of mantle-crust interactions, are examined using constraints imposed by melting experiments, melting-assimilation experiments and Sr-Nd isotope systematics. The Sr-Nd isotope relationships indicate the existence of different genetic trends in which juvenile mantle materials are involved by different mechanisms: (1) a source trend, traced by a particular evolution of the pre-Hercynian basement and indicating mantle participation at the time of sedimentation; (2) a set of magmatic trends traced by gabbro-tonalite-enclave-granodiorite associations, implying the incorporation of new mantle material at the time of granite generation. These relationships strongly support a pure crustal origin for the peraluminous leucogranites, derived from partial melting of crustal protoliths, and a hybrid origin for the peraluminous granodiorites. These granodiorites are the most abundant granitic rocks of the Central Iberian zone (CIZ) of the Iberian massif, implying that processes of hybridisation by assimilation and/or magma mixing played an important role in granitoid production during the Hercynian orogeny. These hypotheses have been tested by means of melting and assimilation experiments. Melting experiments in the range 800–900 °C and at pressures of 3, 6, 10 and 15 kbar indicate that: (1) several potential source materials such as Bt-Ms gneisses and metagreywackes are suitable for the production of peraluminous leucogranite melts; (2) the melt compositions are always leucogranitic, regardless of pressure; (3) pressure exerts a strong influence on the fertility of the source: experiments at 3 kbar produce more than 20 vol% of melt, compared with less than 5 vol% of melt produced at 10 and 15 kbar and at the same temperature. The melting-assimilation experiments carried out at 1000 °C and 4, 7 and 10 kbar and using a proportion of 50% gabbro and 50% gneiss give high melt proportions (more than 50 vol.%) and noritic residues. These melts have the composition of leucogranodiorites, and overlap with part of the compositional range of peraluminous granodiorites of the Iberian massif. The generation of more mafic granodiorites may be explained by the incorporation of some residual orthopyroxene to the granodiorite magmas. The low solubility of Fe + Mg prevents the generation of granodiorite melts with more than 3 wt% of MgO + FeO at all crustal pressures. The large volumes of peraluminous, hybrid granodiorites, produced by assimilation of crustal rocks by mantle magmas, imply that an important episode of crustal growth took place during the Late-Palaeozoic Hercynian orogeny in the Iberian massif.

A. Castro (✉) · J.D. de la Rosa · M. El-Biad
Department of Geology, University of Huelva,
Campus de La Rábida, E21819 Huelva, Spain;
Fax: +34 959 53 0175; E-mail: dorado@uhu.es

A.E. Patiño Douce
Department of Geology, University of Georgia,
Athens, 30602 GA, USA

L.G. Corretgé
Department of Geology, University of Oviedo,
Arias de Velasco s/n, Oviedo, Spain

H. El-Hmidi
High-Pressure Experimental Unit, Department of Geology,
University of Huelva, Campus de La Rábida,
E-21819 Huelva, Spain

Editorial responsibility: W. Schreyer

Introduction

Since the Archaean, granite magmatism has been by far the most important mechanism accounting for heat and mass transfer processes within the continental crust. However, crustal recycling is not the only process involved in the generation of granite melts. Isotope relationships are in many cases indicative of the participation of mantle components incorporated in the granite magmas and/or in their sources at different times in their geological histories. The Iberian massif (Spain

and Portugal) offers a good opportunity to study the processes involved in granite production during orogenic processes. A wide variety of granite types with differences in their chemistries and field relationships were emplaced during the Hercynian orogeny in this massif, specially in the Central Iberian zone on which the present study is focused. Peraluminous leucogranites appear generally associated to high-grade metamorphic areas, but also forming epizonal plutons. Biotite-rich and cordierite-bearing granodiorites and monzogranites are the most abundant granitic rocks of this sector of the Iberian massif. These granodiorites contain mafic microgranular enclaves and are associated to small bodies of basic rocks with which they show magma mingling and mixing relationships. Isotope compositions suggest that mantle components are present in the Iberian granodiorites and in similar peraluminous granodiorites and monzogranites around the world (cf. Collins 1996; Holden et al. 1987; Kagami et al. 1991; Pankhurst et al. 1988; Allègre and Ben Othman 1980). However, the nature of these components, whether inherited from the source or added to the source region at the time of granite generation, is still a matter of debate. Previous experimental work (Patiño Douce 1995; Montel and Vielzeuf 1997) has shown that granodiorites are too calcic to be derived from pelitic sources and too potassic to be derived from amphibolite sources. Only in special circumstances (wet melting of granite gneisses, e.g. Patiño Douce and Beard 1995) and/or using special lithologies (quartz-rich amphibolites, *op. cit.*) it is possible to obtain granodiorite melts at low melting ratios. In the Iberian massif this problem on the origin of peraluminous granodiorites and related monzogranites is particularly relevant as they represent more than 80% of the outcropping granites in the Central Iberian zone (CIZ) and are likely to have been the most important components of Hercynian crustal growth.

In this study we address the origin of common Hercynian granitoids of the CIZ by means of isotopic analyses, melting experiments of likely source materials, and reaction experiments that model the assimilation of crustal source materials by mantle-derived mafic magmas.

Overview of the Iberian granites

The Hercynian granitoids of Iberia (Spain and Portugal) can be subdivided, on the basis of their relationships to the main deformation events, into: (1) *older*, syn-tectonic granitoids; (2) *younger*, post-tectonic granitoids (Schermerhorn 1956; Oen 1958, 1970). The largest volumes of granite magmas are late with respect to the main deformation phases, and are possibly related to crustal-scale extensional processes (Casquet et al. 1988; Doblas 1991). Serrano Pinto (1983) and Serrano Pinto et al. (1987) distinguished several groups of Hercynian granitoids based on their ages, ranging from Devonian to Permian. If ages and structural relationships are considered together, two distinct groups are apparent, one of them showing ages older than 300 Ma and the other displaying ages younger than 290 Ma. These two groups correspond, respectively, to the "older" and "younger" granites mentioned above.

Based on their chemical and mineralogical compositions, Capdevila et al. (1973) and Corretgé et al. (1977) grouped the Hercynian granitoids of the CIZ, both older and younger, into three families: (1) peraluminous, two-mica granites and leucogranites; (2) biotite-granodiorites; (3) cordierite-monzogranites.

Peraluminous, two-mica granites and leucogranites (mostly older)

Almost all these granitoids were intruded between 310 and 330 Ma. They frequently have pelitic inclusions and abundant alumina-rich minerals. They have very low CaO contents, variable $(^{87}Sr/^{86}Sr)_i$, widely variable $(^{147}Sm/^{144}Nd)_i$ ratios (Beetsma 1995), and no HREE (heavy rare earth element) depletion. They display limited geochemical variability in comparison with the biotite granitoids. Almost all anatectic autochthonous, para-autochthonous and allochthonous granites, related in space and time to Hercynian regional metamorphism, are included within this broad group of peraluminous, two-mica granites and leucogranites.

Biotite-granodiorites (mostly younger)

Two groups can be distinguished: "early" granodiorites and "late" granodiorites. Early granodiorites display a large petrographic variety, ranging from granodiorites to K-feldspar megacryst monzogranites. Several types of gabbros, diorites and ultramafic rocks frequently appear intruded by or intruding into the main granodiorite sequence. They display smaller variations of the $(^{147}Sm/^{144}Nd)_i$ ratio (Beetsma 1995) than the peraluminous two-mica granitoids and leucogranites.

Cordierite-monzogranites

They show intermediate features between the other two groups. They share with the group of biotite-granodiorites the presence of microgranular enclaves, the high-K content and low initial Sr isotope ratios. They share with the other group the strongly peraluminous character.

Geology of selected areas and studied rocks

In order to understand the origin and evolution of the Hercynian granitoids we have studied two selected areas of the Central Iberian zone (CIZ, Fig. 1): (1) The Central Extremadura batholith (CEB), that belongs to the epizonal domains of the CIZ and in which leucogranites, monzogranites and biotite-tonalites appear forming uprooted plutons. (2) The Piedrahita-Barco area (PBA), that be-

longs to the deep-seated domains of the CIZ and in which the leucogranites appear associated with anatectic complexes and the granodiorites show magma mingling zones with basic rocks.

Geological details of these areas may be found in Corretgé (1971), Castro (1986), Corretgé et al. (1985), Castro and Fernández (in press) and Vigneresse and Bouchez (1997) for the CEB, and in Pereira (1992) and Pereira and Bea (1994) for the Piedrahita-Barco area.

All the exposed granites in the Central Extremadura area may be grouped into three main categories: (1) biotite-tonalites; (2) cordierite-monzogranites; (3) two-mica leucogranites. Cordierite-monzogranites form concentrically zoned plutons, with the most granitic facies located at the cores of the plutons. Occasionally the marginal facies contain scarce microgranular enclaves. Biotite-rich (surmicaceous) spots (up to 4 cm) are common in the two-mica granites in which microgranular enclaves are absent. Finally, the tonalites are medium-grained, biotite-rich rocks. They have scarce microgranular enclaves and biotite-rich (surmicaceous) spots.

In the Piedrahita-Barco area we have focused on two main granite complexes: (1) the gabbro-granodiorite complex of Puente

Fig. 1 Geological maps of the areas considered in this study and their locations in the Iberian massif (zonal division according to Julivert et al., 1974). *Labels* are key references to samples of Tables 1 and 2

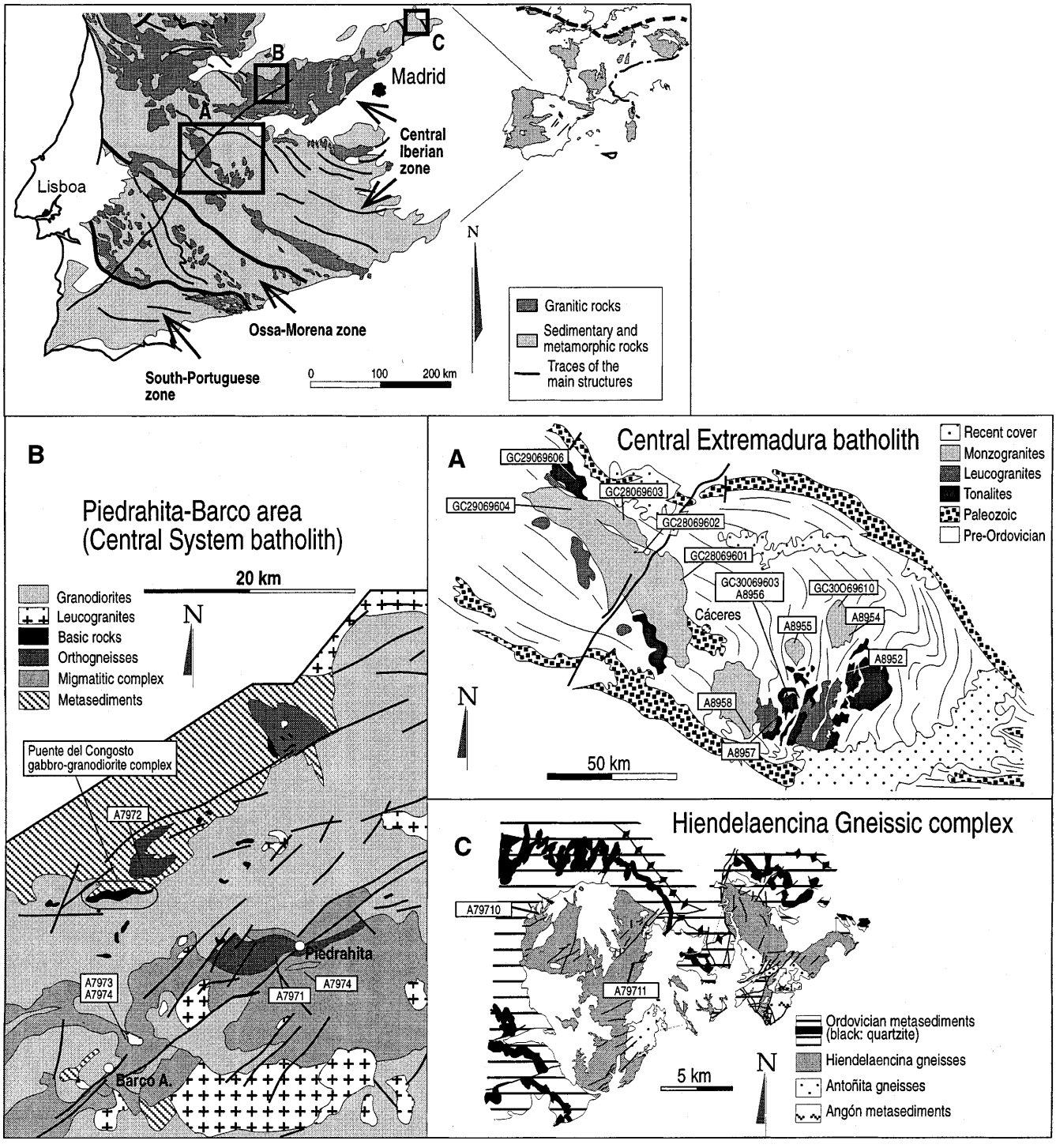

del Congosto; (2) the Peña Negra anatectic complex. A preliminary study of the relationships between granodiorites and mafic rocks in the Puente del Congosto complex was reported by Fernandez et al. (1997). These are indicative of commingling at the level of emplacement between gabbros and granodiorites. Syn-plutonic dikes of mafic magma, enclaves, transitional contacts and intermediate rocks around the gabbro bodies are the main aspect of this complex. Representative samples of the main lithologies were selected for isotope analysis (De la Rosa JD, Rogers G, Castro A in preparation) and assimilation experiments. Apart from the Biotite-rich granodiorites appearing in Puente del Congosto, we have included in this study a few representative samples of typical cordierite granodiorites and monzogranites from the Central System batholith.

In the study of the Peña Negra anatectic complex we have followed the detailed descriptions of Pereira (1992) and Pereira and Bea (1994) to select the main lithologies that may have relevance to the origin of the granitoids, in order to perform isotopic analyses and melting experiments. In summary these lithologies are: (1) granodiorite orthogneiss (La Almohalla gneiss); (2) migmatites and anatectic granites. The first is a pre-Hercynian biotite-granodiorite strongly foliated and folded. The melanosomes of the migmatite complexes are composed of biotite and sillimanite forming relict folds (second deformation phase). Cordierite is very abundant in leucosomes and melanosomes. The leucosomes are composed of leucogranite with magmatic cordierite as the only ferromagnesian phase (Pereira 1992; Pereira and Bea 1994). They appear to be heterogeneous, autochthonous granites forming large pods surrounded by pelitic migmatites.

Potential crustal protoliths

Potential crustal protoliths have been collected from metasedimentary and metavolcanosedimentary formations that are widespread in the Central Iberian zone. These are: the Ollo de Sapo gneiss, and equivalents in high-grade zones (Bercimuelle gneiss), and greywackes of the Lower Cambrian/Upper Precambrian schist-greywacke complex. The Ollo de Sapo gneiss has long been considered a potential source material for many Iberian granites (e.g. Ortega and Gil Ibarguchi 1990). It outcrops in the north of the Central Iberian zone, in Galicia and in the Central System. The protolith for this formation is a matter of debate and it is beyond the scope of this paper. Field relationships, textures and geochemistry favour a volcanosedimentary origin for most of the rocks that make up the formation. In low-grade zones this rock is composed of more than 30 vol.% of micas. In high-grade zones the same rock may be very rich in K-feldspar, giving a more granitic appearance. We refer to these rocks as biotite-muscovite-gneisses in order to avoid confusion on their possible provenance. The U-Pb dating of zircons by Lancelot et al. (1985), yields an age for the Ollo de Sapo in the north-western part of the Iberian Massif of between 500 and 600 Ma (Upper Precambrian to Cambrian). The U-Pb ages of zircons in the Hiendelaencina area give a minimum age of about 550 Ma (Lower Cambrian) according to Wildberg et al. (1989).

The samples of the Ollo de Sapo gneiss that we have selected for this study come from the Hiendelaencina region (Fig. 1). We have used the detailed maps and descriptions by Fernandez (1991) to select the most representative samples. One of these is a coarse-grained augen gneiss with K-feldspar megacrysts up to 10 cm long. The matrix is essentially composed of quartz (Qtz), biotite (Bt), muscovite (Ms) and plagioclase (Pl) (An_{10}). This facies is ideal for melting experiments because the water contained in Bt and Ms is likely to be the water that the rock contains at the beginning of melting in nature. The other representative sample collected from the Hiendelaencina area is a fine-grained facies of the same augen gneiss. The chemical composition of this facies is very similar to that of the coarser grain one.

The Bercimuelle gneiss is a coarse-grained foliated rock composed of Kfs megacrysts in a matrix of Qtz, Pl (An_{10-15}), Bt, Crd (cordierite) and Sil (sillimanite). It belongs to a series of high-grade metamorphic rocks from SE Salamanca (Fig. 1). This rock is used in the melting experiments and the results contrasted with those of the Ollo de Sapo samples. Both rocks are similar in major element compositions but the Bercimuelle gneiss is very rich in cordierite, and thus depleted in water relative to Ollo de Sapo.

Finally, greywackes are the most abundant rocks in the Lower Cambrian/Upper Precambrian terrigenous series of the Central Iberian zone (Fig. 1). They form a thick (2–6 km) monotonous succession alternating with shales. These greywackes contain a high proportion of volcanoclastic material (Rodriguez Alonso 1985), which must be considered in the petrogenetic modelling (cf. Nägler et al. 1995). Ortega and Gil Ibarguchi (1990) consider these greywackes to be among the source materials for the Hercynian granites, according to the results of the REE-based geochemical modelling. For our partial melting experiments we have selected samples of metagreywackes from the metamorphic aureole of the Alburquerque granite in Central Extremadura. These aureole rocks have lost all the chlorite and are rich in cordierite and biotite. Consequently, they have a water content lower than the chlorite-rich metagreywackes that appears in the low-grade areas, which is possibly closer to the water content that they were likely to have at the beginning of partial melting.

Analytical methods and results

Representative samples from the granites, anatectic complexes and potential protoliths have been analysed for major and trace elements as well as for Sr and Nd isotopes. Sample locations are shown in Fig. 1. Major elements were determined by XRF at the University of Oviedo. Isotopic analyses were performed at the University of Granada according to the procedure of Montero and Bea (1998) for Rb, Sr, Sm and Nd determinations by ICP-MS. The Rb and Sr were separated using BIORAD AG 50 W8 ion-exchange resins. Analytical determinations were performed in a Finnigan MAT 262 thermal ionisation mass-spectrometer, with a precision better than 0.0028% (2 sigma), calculated from repeated measurements of the WSE standard. The accuracy calculated on repeated measurements of the NBS-987 standard is better than 0.0007% (2 sigma). The normalising value for $^{87}Sr/^{86}Sr$ is $^{88}Sr/^{86}Sr = 8.375209$. A similar method was used for Nd isotope determinations. The normalisation value for $^{143}Nd/^{144}Nd$ is $^{146}Nd/^{144}Nd = 0.7219$. The accuracy calculated on repeated measurements of the La Jolla standard is better than 0.0018% (2 sigma).

Results of the chemical and isotopic study

Tables 1 and 2 show, respectively, chemical and isotopic data of representative samples from the granitic rocks and potential source materials discussed in this study. Variations in major elements are summarised by the A-B multicationic diagram (De la Roche 1978; Debon and Le Fort 1983), in which the factor A is the Al saturation index and the factor B is the sum of Fe + Mg + Ti, which reflects the content of ferromagnesian phases (Bt, Amp, Px, etc.). The following observations can be made (Fig. 2):

1. Leucogranites, monzogranites and tonalites of the Central Extremadura batholith (CEB) display a trend comparable to other granite associations of the Iberian massif.

2. The composition of the leucosomes from the Peña Negra anatectic complex plot in the "leucogranite" field overlapping most of the leucogranite massifs.

3. Peraluminous migmatites, and gneisses (Ollo de Sapo and Bercimuelle) plot away from the trend of

Table 1 Geochemical analyses of representative samples from granites and source materials. Mineral abbreviations from Kretz (1983). (*LOI* loss on ignition)

Sample	Rock type	Locality	Refer to Fig. 2	SiO_2	TiO_2	Al_2O_3	Fe_2O_3	MnO	MgO	CaO	Na_2O	K_2O	P_2O_5	LOI	Total
Tonalites from the Central Extremadura batholith															
A8952	Bt-tonalite	Santa Cruz		65	0.66	16.7	4.37	0.05	1.82	3.47	3.64	2.5	0.21	0.6	99.02
A8956	Bt-tonalite	Zarza Mont.		72	0.24	14.7	2.43	0.04	0.78	1.8	3.79	2.87	0.16	0.5	99.31
GC29069606	Bt-tonalite	Zarza Mayor		67.8	0.51	16.1	3.7	0.03	1.5	2.76	3.79	2.57	0.2	0.75	99.71
Monzogranites from the Central Extremadura batholith															
A8954	2-mica granite	Trujillo		72.8	0.2	14.6	1.8	0.02	0.72	0.66	3.63	4.24	0.44	0.85	99.96
GC30069610	Crd-monzogranite	Trujillo		71.7	0.26	15.1	2.01	0.03	0.41	0.95	3.78	4.64	0.37	0.45	99.7
A8958	Crd-monzogranite	Alcuescar		72.3	0.3	14.8	2.24	0.03	0.49	1.02	3.55	4.33	0.3	0.45	99.81
GC28069601	2-mica granite	Cabeza Araya		73.2	0.28	14.4	2.1	0.01	0.45	0.83	3.29	4.46	0.31	0.5	99.83
GC28069602	Crd-monzogranite	Garrovillas		70.1	0.44	15	2.7	0.01	0.74	0.84	3.51	5.16	0.31	0.75	99.56
GC28069603	Crd-monzogranite	Garrovillas		70.7	0.43	14.4	2.71	0.02	0.57	1.21	3.47	4.79	0.35	0.35	99
Leucogranites from the Central Extremadura batholith															
A8955	Leucogranite	Plasenzuela		73.4	0.09	14.9	1.22	0.03	0.21	0.48	3.89	4.47	0.5	0.75	99.94
A8957	Leucogranite	Montánchez		73.7	0.09	14.7	1.08	0.02	0.14	0.5	4.07	4.04	0.64	0.55	99.53
Anatectic granites from the Piedrahita-Barco area															
A7973	Crd granite	Barco de Avila	3	72.68	0.13	15	1.46	0.02	0.29	0.47	3.54	5.44	0.33	0.82	100.18
A7979	Crd leucogranite	Peña Negra	9	72.16	0.19	14.91	1.76	0.02	0.54	0.38	2.14	7.06	0.18	0.77	100.11
Cordierite granodiorites from the Gredos area															
A7975	Granodiorite Crd layer	Gredos	5	68.54	0.51	15.52	4.18	0.07	1.48	1.02	2.49	4.8	0.12	1.13	99.86
A7976	Granodiorite Bt layer	Gredos	6	64.15	0.98	16	6.24	0.07	1.97	2.12	3.4	3.82	0.27	0.99	100.01
A7977	Granodiorite Crd layer	Gredos	7	71.4	0.29	15.05	2.65	0.05	0.94	1.07	2.56	5.16	0.14	0.96	100.27
Potential source materials															
A7971	Crd-Bt gneiss	La Almohalla	1	67.02	0.41	16.98	3.18	0.04	0.6	3.18	4.09	3.62	0.2	0.59	99.91
A7972	Bt-gneiss	Bercimuelle	2	68.6	0.48	15.69	3.99	0.07	1.36	0.87	2.82	4.56	0.23	1.26	99.93
A7974	Migmatite	Barco	4	76.38	0.65	10.98	4.76	0.04	1.55	0.48	1.21	1.87	0.06	1.94	99.92
A79710	Bt-Ms gneiss	Hiendelaencina	10	69.1	0.52	15.23	4.19	0.04	1.51	1.28	3.06	3.81	0.18	1.3	100.22
A79711	Bt-Ms gneiss	Hiendelaencina	11	71.58	0.37	14.53	3.44	0.06	1.28	0.87	2.62	4.2	0.14	1.21	100.3
IT516	Metagreywacke	Extremadura		62.75	0.83	16.95	7.7	0.05	2.69	0.19	1.85	3.62	0.14	3.11	99.88
IT521	Metagreywacke	Extremadura		69.81	0.7	13.67	5.84	0.04	1.59	0.18	2.69	2.06	0.15	3.19	99.92
Puente del Congosto gabbro															
A119648	Gabbro	P. Congosto		50.09	0.59	12.38	10.33	0.15	15.13	6.25	1.72	1.41	0.14	1.82	98.98

Table 2 Isotope analyses of representative samples from granites and source materials. Mineral abbreviations from Kretz (1988)

Sample	Rock type	Refer to Fig. 3	Locality	Rb (ppm)	Sr (ppm)	$^{87}Rb/^{86}Sr$	$^{87}Sr/^{86}Sr$
Tonalites							
A8952	Tonalite bt	1	Santa Cruz	92.3	160.1	1.669	0.71619
A8956	Tonalite bt	3	Zarza de Montánchez	99.4	89.4	3.224	0.72676
GC29069606	Tonalite bt	4	Zarza la Mayor	96.3	150.3	1.856	0.71878
Serie Mixta							
A8954	Granite 2 micas	5	Trujillo	334.7	36.1	27.200	0.83946
GC30069610	Monzogranite	6	Trujillo	266.8	59.4	13.076	0.76748
A8958	Monzogranite	7	Alcuescar	236.4	73.3	9.363	0.74822
GC28069601	Granite 2 micas	8	Cabeza Araya	220.9	51.6	12.453	0.76372
GC28069602	Monzogranite	9	Garrovillas	157.6	59.5	7.691	0.74457
GC28069603	Monzogranite	10	Garrovillas	180.9	58.5	8.989	0.75076
Leucogranites							
A8955	Leucogranite	13	Plasenzuela	184.7	18.3	29.784	0.89068
A8957	Leucogranite	14	Montánchez	216.7	44.0	14.381	0.80534
Anatectic granitoids							
A7973	Crd nodule granodiorite		Barco de Avila	182.9	63.8	8.295	0.75814
A129719	Crd leucogranite		Peña Negra	161.3	142.4	3.278	0.73273
A7979	Migmatite		Peña Negra	224.3	241.7	2.687	0.72907
Cordierite granodiorite							
A7975	Granodiorite-Crd layer		Gredos	236.1	197.3	3.464	0.72612
A7976	Granodiorite-Bt layer		Yuste	316.9	200.4	4.577	0.72697
A7977	Granodiorite-Crd layer		Yuste	214.4	189.2	3.278	0.72231
Sources							
A7971	Gneiss Bt (granodiorite)		Piedrahita	99.8	212.1	1.361	0.71596
A7972	Gneiss Bt-Sill		Bercimuelle	207.9	91.0	6.610	0.75569
A7974	Migmatite		Barco de Avila	126.4	93.0	3.933	0.73142
A79710	Ollo de Sapo coarse grain		Bustares	159.6	139.7	3.305	0.73145
A79711	Ollo de Sapo fine grain		Hiendelaencina	118.3	107.3	3.190	0.73341
IT516	Greywacke		Extremadura	133.5	65.8	5.866	0.75005
IT521	Greywacke		Extremadura	78.0	52.7	4.285	0.73970

granites. Only the Crd-rich bands of the heterogeneous granodiorites of Gredos plot close to the Ollo de Sapo and migmatitic gneisses (e.g. Bercimuelle). Similar results were reported for these Crd-bearing granodiorites by Moreno Ventas et al. (1995).

Figure 3 shows a Rb-Sr isotope plot for the Central Extremadura granites. Cordierite-monzogranites and Bt-tonalites fit to a regression line giving an age of 326 ± 24 Ma and an initial $^{87}Sr/^{86}Sr$ ratio of 0.7088. This correlation is good even if the more radiogenic sample, that corresponds to a two-mica granite from Trujillo, is not considered. The points on this diagram correspond to representative samples from different plutons, which are not obviously related by processes of magmatic differentiation. However, the observed correlation mimics the behaviour of a closed chemical system, at least for Sr. The meaning of this apparent paradox will be discussed later. The two samples of leucogranites correspond to the plutons of Montanchez and Plasenzuela and these are outside of the main trend.

Figure 4 shows all the samples analysed in this study in an ε_{Nd} versus Sr initial ratio diagram, calculated for 300 Ma. This is a reference age for the main magmatic and metamorphic processes during the Hercynian orogeny. The monzogranite-tonalite samples of the Central Extremadura batholith plot along a curvilinear trend, pointing on one end towards a mantle end-member and on the other end towards a crustal source. A similar pattern is defined by the samples of the gabbro-granodiorite complex of Puente del Congosto. Samples collected from potential source materials plot along a different trend. The origin of this source trend will be discussed later. Hybrid granodiorites from the Gredos area plot within the lower-right quadrant in a triangle bound between the source trend and the lines of CHUR (chondrite uniform reservoir) composition. These results are in agreement with those of Moreno-Ventas et al. (1995) and Villaseca et al. (1998) for similar rocks from the Gredos massif.

Hypothesis on the origin of the CIZ granites

Sr-Nd isotopic features of potential source materials: the source trend

The data presented in this paper on crustal source materials, together with those of Ugidos et al. (1997a, b), define a positive trend on an ε_{Nd} versus Sr initial ratio diagram (Fig. 4). The positive slope of this "source trend" may appear to be paradoxical and requires an explanation. The key to this explanation resides in the different behaviours of the Rb-Sr and Sm-Nd pairs

2σ	$^{87}Sr/^{86}Sr_{300}$	Sm (ppm)	Nd (ppm)	$^{147}Sm/^{144}Nd$	$^{143}Nd/^{144}Nd$	2σ	$^{143}Nd/^{144}Nd_{300}$	$\varepsilon_{Nd3_{00}}$	T_{DM}
2	0.70907	5.4	25.6	0.1280	0.512418	12	0.512167	−1.7	1.15
2	0.71300	2.5	10.7	0.1422	0.512431	17	0.512152	−2.0	1.17
3	0.71086	5.8	26.5	0.1312	0.512499	15	0.512241	−0.2	1.04
2	0.72334	3.1	14.4	0.1293	0.512319	14	0.512065	−3.6	1.31
2	0.71165	3.5	16.9	0.1250	0.512372	20	0.512127	−2.4	1.21
2	0.70825	3.9	19.0	0.1244	0.512422	20	0.512178	−1.4	1.13
2	0.71055	3.6	16.2	0.1352	0.512455	20	0.512190	−1.2	1.12
5	0.71174	4.5	20.1	0.1360	0.512408	20	0.512141	−2.2	1.19
5	0.71238	5.3	24.0	0.1324	0.512359	16	0.512099	−3.0	1.26
4	0.76353	0.9	3.2	0.1766	0.512422	20	0.512075	−3.4	1.29
3	0.74395	1.0	3.4	0.1846	0.512423	20	0.512061	−3.7	1.21
5	0.72272	1.4	5.9	0.1483	0.512310	20	0.512019	−4.5	1.38
2	0.71874	4.9	23.9	0.1263	0.512025	8	0.511777	−9.3	1.74
3	0.71760	2.3	11.5	0.1204	0.512013	16	0.511777	−9.3	1.75
2	0.71133	5.9	34.5	0.1041	0.512075	15	0.511871	−7.4	1.61
4	0.70743	10.6	61.1	0.1044	0.512168	12	0.511963	−5.6	1.46
3	0.70831	3.6	20.0	0.1088	0.512058	50	0.511844	−8.0	1.65
2	0.71015	13.0	64.7	0.1210	0.512358	17	0.512120	−2.6	1.22
2	0.72747	6.0	27.9	0.1292	0.512244	12	0.511990	−5.1	1.42
3	0.71463	5.9	31.2	0.1133	0.512488	16	0.512265	0.3	1.00
2	0.71734	6.4	30.8	0.1265	0.512190	15	0.511942	−6.1	1.50
2	0.71979	4.2	19.7	0.1294	0.512216	14	0.511962	−5.7	1.47
2	0.72500	5.9	29.2	0.1213	0.512214	14	0.511976	−5.4	1.41
2	0.72140	5.3	25.3	0.1259	0.512229	17	0.511982	−5.3	1.41

during surface processes of weathering and sedimentation (cf. Taylor and McLennan 1985). The Sm-Nd pair is essentially not fractionated by processes that take place at the surface of the Earth. In contrast, Rb is incorporated and adsorbed by clay minerals, and hence trapped in sediments, whereas Sr is leached by aqueous fluids and eventually accumulates in the oceans. A consequence of these different behaviours is that the Sr isotopic compositions of pelitic sediments are very sensitive to incorporation of even small amounts of juvenile mantle material, whereas their Nd isotopic compositions are more robust. This is illustrated in Fig. 5, which shows model mixing lines between a typical mantle end-member and three putative sedimentary rocks. Mixtures with 50% or more of mantle material have Nd isotopic compositions that are virtually indistinguishable from those of the crustal end-member, and Sr isotopic compositions that are much more variable but which, in any case, are closer to that of the mantle end-member than to that of the crustal end-member. The subhorizontal trends in ε_{Nd} versus Sr initial ratio diagrams that are often observed in metasedimentary sequences (such as the metagreywackes and volcano-sedimentary gneisses of the Ollo de Sapo Formation, e.g. Beetsma 1995) can thus be explained as arising from mixing of varying amounts of crustal and mantle end-members of nearly constant compositions. The positive slope of the source trend in Fig. 4 suggests that the likely metasedimentary sources of the Iberian granitoids include several different crustal end-members, and that these have been mixed with varying proportions of juvenile mantle materials (see Fig. 5). Mixing between crustal and mantle materials must have taken place at the time of sedimentation because: (1) if the mantle materials had been present in the source area of the sediments, then Sr would have been leached from them too, and they would not give rise to the observed mixing trend; (2) if the mantle materials were younger than the sediments, then they would be recognisable petrographically as discrete intrusive and/or extrusive units, which are virtually unknown in the Iberian metasediments. The most likely alternative is, then, that the mantle material was incorporated into the sediments at the time of sedimentation, as mineral and rock fragments of volcanic origin that were not significantly weathered and that therefore retained their original Sr contents.

Hypothesis on the origin of the peraluminous leucogranites

Peraluminous leucogranites match the major element composition of migmatite leucosomes (Crd-leucogranites, see Table 1, and Fig. 2). Field relationships observed in anatectic complexes such as those in the Piedrahita-Barco area (e.g. Pereira 1992; Pereira and Bea 1994), suggest in-situ segregation of granitic melts from pelitic migmatites within the stability field of Crd.

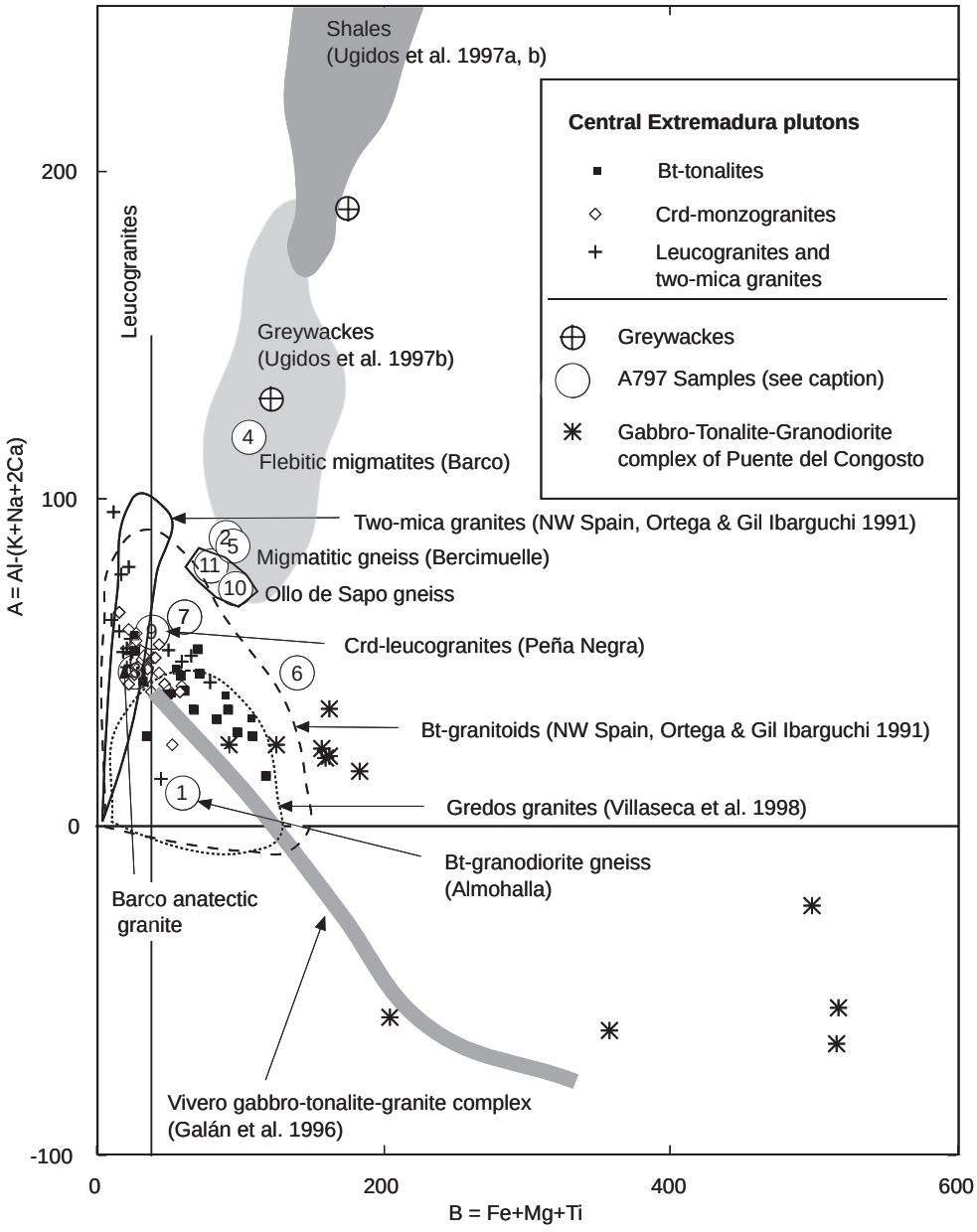

Fig. 2 A-B multicationic diagram (Debon and Le Fort 1983) showing the position of granites, basic rocks and potential source materials studied in this paper and the position of the Lower Cambrian/Upper Precambrian greywackes according to data of Ugidos et al. (1997a, b). *Numbers inside circles* correspond to samples A797 (Table 1) [*1* La Almohalla gneiss, *2* Bercimuelle gneiss; *3* anatectic granite (Barco); *4* flebitic migmatite (Barco), *5*, *6*, *7* Gredos cordierite-rich granodiorites, *9* Piedrahita migmatites (leucosomes), *10* and *11* Ollo de Sapo gneisses (Hiendelaencina)]

The relationships displayed by leucogranites in the ε_{Nd} versus Sr initial ratio diagram indicate that: (1) they have been generated from a pure crustal protolith; (2) no single source material accounts for the generation of all peraluminous leucogranites in the Iberian massif. The isotopic ratios of peraluminous leucogranites match the ratios of different crustal protoliths along the source trend. A similar result was obtained by Villaseca et al. (1998) comparing the Sr-Nd isotope ratios of peraluminous granites and orthogneisses of the Central System batholith. Our data and those of Villaseca et al. (1998) show that peraluminous leucogranites with virtually identical major and trace element compositions can have widely variable Sr and Nd isotopic ratios. This reflects the fact that leucogranite melts are eutectic-like compositions, so that dehydration melting of different micaceous protoliths yields melts within a very restricted compositional range (Patiño Douce and Johnston 1991; see also Montel and Vielzeuf 1997). We further test this hypothesis with melting experiments of several possible source matarials for the Iberian peraluminous leucogranites.

Hypothesis on the origin of peraluminous granodiorites and monzogranites. Mixed source, magma mixing or assimilation?

The Sr and Nd isotopic compositions show that a juvenile mantle component is present in many peraluminous granodiorites and monzogranites (Fig. 4). This figure also shows that at least part of the mantle con-

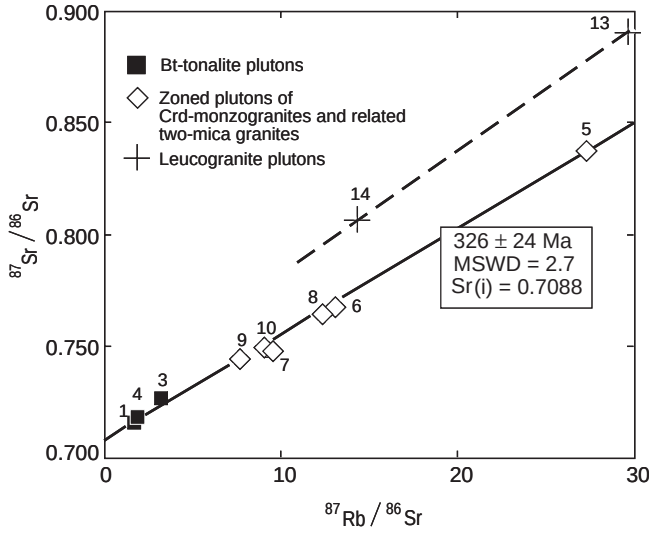

Fig. 3 Rb-Sr isotope correlation between granitic rocks of the Central Extremadura batholith. *Labels over the symbols* in the Extremadura plutons correspond to samples in Table 2

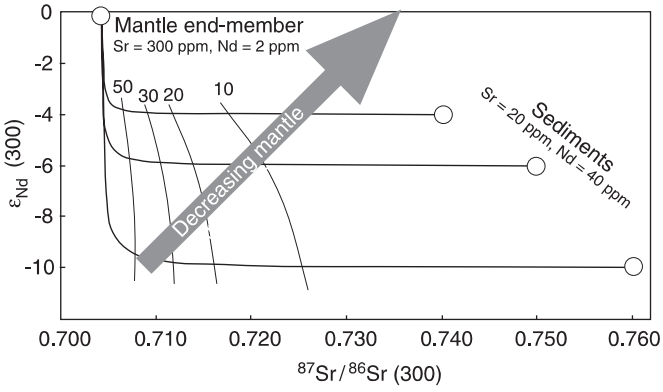

Fig. 5 Model mixing lines calculated for three different crustal end-members and a common mantle end-member. The diagram illustrates the possible generation of the positive source trend displayed by source samples in Fig. 4. This source trend implies that the participation of mantle material in the source at the time of sedimentation was decreasing with time. The Sr and Nd concentrations in mantle and crust make the epsilon Nd a marker of the crustal residence time (model age) and the Sr initial ratio a measure of the mantle participation at any time (see text). *Labeled curves* represent isopleths (in %) of the mantle components in the mixture

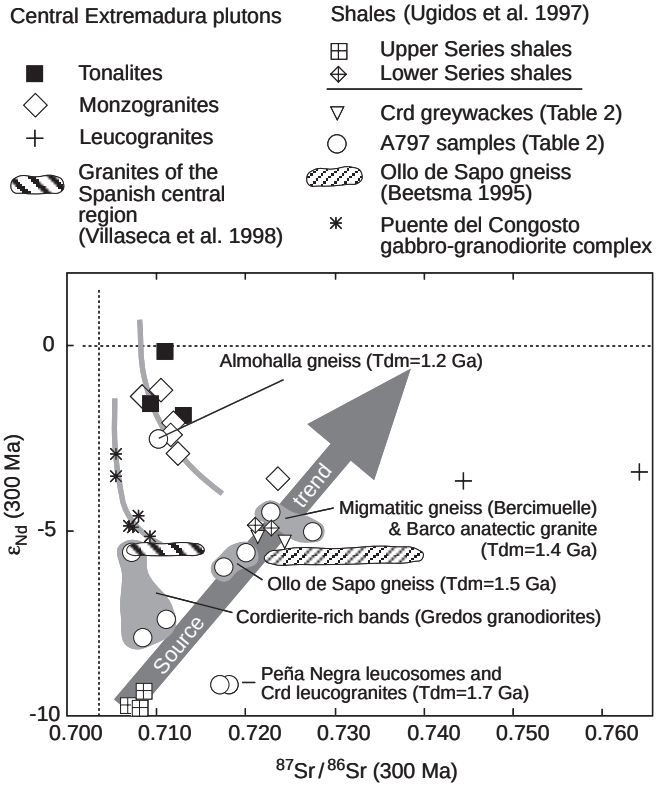

Fig. 4 Epsilon (Nd) versus Sr initial ratio diagram plotting representative samples of granite complexes and crustal protoliths of the Central Iberian zone. Granites display curvilinear (hyperbolic) trends linking a mantle end-member and more than one crustal end-member. Crustal end-members are disposed along a "source trend" following a positive evolutionary line in the *lower right quadrant* of the plot. The origin and implications of this source trend is explained in the text. All data have been recalculated to a reference age of 300 Ma

tribution occurred at, or very close to, the time of magma generation. We argue that the process responsible for this was assimilation of crustal rocks by basaltic magmas (e.g. Patiño Douce 1995). Other possible processes include melting of mixed crustal sources, melting of hybrid metaigneous compositions, and mixing of anatectic melts with mantle-derived magmas. There are arguments, however, that suggest that neither of these processes was important in the origin of the peraluminous granodiorites and monzogranites of the Iberian massif.

The mixed crustal source model can be discarded because such sources (interlayered amphibolites and pelites) are unknown in the Iberian massif and, furthermore, because the experimental results of Skjerlie and Patiño Douce (1995) suggest that rates of melt extraction are likely to be faster than diffusive homogenization among layers, hampering the generation of large volumes of compositionally homogeneous hybrid melts.

Melting of hybrid metaigneous sources, such as potassic andesites, was advocated by Roberts and Clemens (1993) as an explanation for the origin of granodiorites with mantle-like isotopic compositions. This model finds some support in the melt compositions produced experimentally from a quartz amphibolite by Patiño Douce and Beard (1995). However, application of this model to the peraluminous granodiorite and monzogranites of the Iberian massif runs into several difficulties. In the first place, such sources are scarce in the Central Iberian zone of the Iberian massif. Second, generation of potassic andesites can only take place by hybridization of mafic magmas with crustal rocks. This means that interaction of mafic magmas with crustal rocks would nevertheless be called upon, but in order to generate putative source materials rather than the

granitoids themselves – in effect "pushing" the problem back one step, rather than addressing it. Also, the residues formed by partial melting of quartz-amphibolites are rich in clinopyroxene (Patiño Douce and Beard 1995), which, if partially entrained in the granitoid magmas (as required by the difference in FeO + MgO contents of natural granitoids relative to experimental melts – see below) would generate metaluminous hornblende-bearing granodiorites, rather than peraluminous granodiorites and monzogranites.

Magma mixing and mingling zones are known in many granitoid massifs (e.g. Moreno Ventas et al. 1995; Galán et al. 1996), but they cannot account for the hybrid isotopic compositions of the entire massifs, because they are always local phenomena that affect only relatively minor volumes of the granitoid complexes, and, most importantly, because the more felsic rocks in the magma mingling zones are already hybrid granodiorites, which clearly must have acquired their hybrid isotopic compositions before reaching the magma mingling zones. Assimilation of crustal rocks by basaltic magmas thus appears to be the most plausible explanation for the generation of large volumes of granodiorites with hybrid isotopic compositions.

The remarkable correlation among the Sr isotopic compositions of different granodiorite intrusions, their enclaves, and related mafic rocks also sheds light on this issue. An example has already been discussed for the granites of the CEB (Fig. 3). A likely explanation for these relationships is that the different plutons of the CEB contain varying amounts of juvenile mantle magma in them that were incorporated at the time of melting. Because of the low Sr content of the crustal sources, this mantle component dominates the Sr isotopic compositions of the granitoids, in effect causing granitoids with different proportions of crustal and mantle components to have virtually the same initial isotopic ratios. This explanation is also applicable to the linear trends obtained for granodiorites and enclaves from other massifs of the European Hercynides (e.g. Ibarrola et al. 1987; Pinarelli and Rottura 1995; Moreno Ventas et al. 1995; Villaseca et al. 1998 in the Spanish Central System; Fourcade and Javoy 1991 in the Pyrenees; Pin 1991; Turpin et al. 1990 in the Massif Central, France). A good example of this is the regression line displayed by the rocks of Puente del Congosto (Fig. 6). These rocks include gabbros, tonalites, enclaves and granodiorites forming part of a magma mingling zone. These relationships can be modelled by a simple binary mixing between a crustal end-member, the Bercimuelle gneiss, and a mantle end-member, the Puente del Congosto gabbro (Fig. 6). Villaseca et al. (1998), on the basis of Sr-Nd isotope ratios, estimated the mantle participation in the granitoids of the Gredos area (Central System) at between 25% and 50%. They considered these results unrealistic, and assumed a pure crustal source for these granitoids. However, their results are in agreement with our assimilation model, in which a 50% of mantle component may be present in the granitoids.

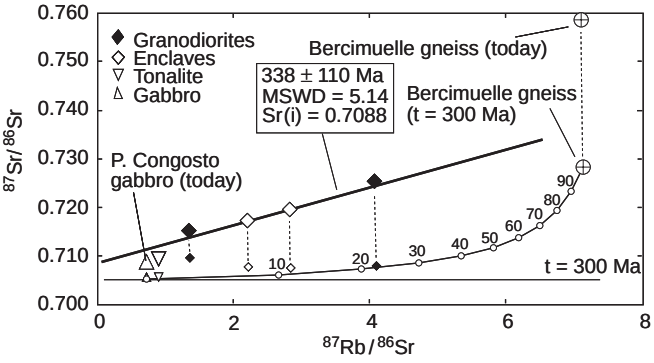

Fig. 6 Isochron obtained for the rocks of Puente del Congosto. All the points were on a *horizontal line* at the time of hybridisation (ca. 300 Ma ago) between a mantle-derived magma and a crustal source. The samples used for the model line are a gabbro of Puente del Congosto (sample A119648) and the Bercimuelle gneiss (sample A7972). This process of hybridisation explains the observed correlation between granites and between granites and enclaves, as well as the low Sr initial ratios that characterise the biotite calc-alkaline granites

Experimental test of the origin of the Hercynian granites of Iberia

In order to test these hypotheses, we have carried out a set of melting and assimilation experiments covering the complete range of pressures of the continental crust and over a temperature range of 800 to 900 °C. Assimilation of crustal protoliths by basalt magmas was studied previously experimentally by Patiño Douce (1995). Here we present a specific application of these melting-reaction experiments to the origin of the Iberian granitoids, using what are likely to be their actual source materials. Tables 1 and 3 show the chemical composition and mineral modes of the starting materials used in this study.

Pressure is likely to be the most important variable controlling melt compositions (e.g. Patiño Douce 1996). The melting experiments reported here were carried out at pressures of 3, 6, 10 and 15 kbar, and at temperatures of 800 and 900 °C. In the assimilation experiments we used a 1:1 basalt-to-crustal rock proportion, at a temperature of 1000 °C, in order to satisfy thermal requirements for assimilation of crustal rocks by basalt magma (Patiño Douce 1995). The aim of these experiments is to try to reproduce the compositions of the hybrid granodiorites that make up much of the Central Iberian zone of the Iberian massif. To cover the complete range of depths at which hybridisation may have occurred, we have performed these experiments at pressures of 4, 7 and 10 kbar.

Experimental procedures and results

Experiments were carried out in end-loaded, solid-media piston-cylinder apparati at the University of Huelva, with 12.7 mm (0.5 inch) diameter NaCl-graphite cell assemblies for experiments at pressures of 6 kbar and greater, or with CaF_2-graphite cell as-

Table 3 Mineral modes of starting materials. *Number in brackets* are : Mg number for Bt, Crd, Opx and Hbl, and mol% of An in Pl. Mineral abbreviations according to Kretz (1983)

Sample	A79710	A7972	A79711	A7971	IT-521	A119648
Rock type	Bt-Ms gneiss (Ollo de Sapo, coarse-grained facies)	Crd-Sil gneiss (Bercimuelle)	Bt-Ms gneiss (Ollo de Sapo, fine-grained facies)	Granodiorite gneiss (La Almohalla gneiss)	Metagreywacke (LowerCambrian/ Upper Precambrian complex)	Gabbro (Puente del Congosto complex)
Modal composition (vol.%)						
Qtz	34	36–40	36	40	54	–
Bt	18 (40)	10–12 (41)	16 (41)	14 (27)	8 (41)	15 (73)
Ms	20	–	16	–	10	–
Pl	22 (5–20)	10–14 (16)	20 (17)	35 (30)	10 (Ab)	33 (51–74)
Kfs	5	26–30	11	10	–	–
Crd	–	8–10 (50)	–	–	8–10 (58)	–
Sil	–	6–8	–	–	–	–
Hbl	–	–	–	–	–	42 (71)
Opx	–	–	–	–	–	7 (72)
Cpx	–	–	–	–	–	< 2
Oxides	< 2	< 1	< 2	< 2	< 1	2

semblies for experiments at lower pressures. Samples were contained in welded Au capsules, 2.4 mm inner diameter with 0.3 mm wall, containing 10 mg of dry sample and, in experiments with added H_2O, the appropriate amount of water was added with a microsyringe. Weight loss in capsules with added H_2O, was monitored during welding, and the capsules were also checked for leaks before the experiments by verifying that no weight loss (± 0.1 mg) occurred after 2 h in an oven at 130 °C. Durations of H_2O -added experiments were less than those of dry experiments, in order to minimise water loss by diffusion through the capsule material (Patiño Douce and Beard 1994). However water favours ionic diffusion, so that these shorter durations are not likely to affect the approach to equilibrium. Capsules were examined for tears and weighed after the experiments. No weight loss was detected in the experiments reported in this paper. It has been demonstrated (Patiño Douce and Beard 1994, 1995) that the graphite-based cell assemblies used in these experiments limit the $f\,O_2$ in the samples to a well defined interval below the QFM buffer (between QFM and QFM-2). The stability and compositions of ferromagnesian phases are not affected by $f\,O_2$ variations within the range imposed by these cell assemblies (Patiño Douce and Beard 1994, 1995), and these $f\,O_2$ conditions are reasonable for deep crustal processes (see Patiño Douce and Beard 1996).

Temperatures were measured and controlled with Pt_{100}-$Pt_{87}Rh_{13}$ thermocouples feeding Eurotherm 808 controllers with internal ice point compensators. Temperature stability during all runs was ± 5 °C. The reported pressures are oil pressures measured with electronic DRUCK PTX 1400 pressure transmitters, feeding OMRON E5CK controllers, multiplied by ratio of ram-to-piston areas, and were manually maintained within ± 5 bar of oil pressure (ca. 250 bar on the sample). Patiño Douce (1995) showed that, using an all-NaCl cell assembly, piston-cylinder experimental pressures are accurate to within 0.5 kbar even at nominal pressures as low as 5 kbar. Extrapolation of this conclusion to 3 kbar remains uncertain. There are consistent differences between our 3 kbar experimental results and those from higher pressure runs that suggest that these very low pressure experiments can, at the very least, provide geologically meaningful results, even if the pressure uncertainty is unknown, and potentially large. Experimental products were mounted in epoxy, sawed in half and polished. Textures were studied in a SEM using BSE images.

Modal compositions and EDS analyses

Modal proportions of glass (quenched melt) and neoformed phases were determined by image analysis using BSE (Z-contrast) images and the INHimage software. The final values are average values from several different windows of the same run. Glass and crystalline phases were analysed using a LINK-ISIS energy-dispersive spectrometer mounted on a scanning electron microscope (JEOL-JSM5410) at the University of Huelva. Conditions were fit to 15 kV accelerating voltage and 100 s of effective counting time. Matrix corrections were made using the ZAF procedures using a combination of silicates, oxides and pure metals as standards (wollastonite for Ca and Si, jadeite for Na, orthoclase for K, corundum for Al, periclase for Mg, metallic Fe and Ti for Fe and Ti).

If the available clean surface of mineral grains or glass was large enough, the analyses were performed rastering the 1 μm beam over an area of about 6 μm^2. This technique minimises Na loss in Pl and glass, and also gives good results for the rest of the elements. Even using this procedure, Na loss from glass is appreciable, and must be corrected by measuring Na contents at 1/3 of the total counting time. We have observed that this is the time at which the counting rate for Na starts to decrease in our hydrated glasses. In runs near the solidus, in which the melt percentage is very low (< 5%), it is necessary to analyse the glass on very small areas using a fixed beam of 1 μm diameter. In this case, Na loss is very pronounced even at 1/3 of the counting time. However, Na loss is a continuous process that can be fit to curves that may be applied to these small area analyses. The method was checked by analysing large areas of glass with both techniques, rastering the beam and fixed beam, and the results were in good agreement. A similar procedure was followed for plagioclase analyses. Analyses of small grains and small glass areas are only indicative because of the large effects of contamination with X-ray from the surrounding grains. In general, glass analyses corresponding to runs with less than 10 vol.% melt are not very accurate.

Results of the experimental study

Melting experiments of crustal sources

Table 4 shows the experimental conditions and phase assemblages in the melting experiments on the different potential source materials listed in Table 3. Textural and chemical features of mineral phases are discussed below, and shown in Fig. 7.

Table 4 Experimental conditions and summarised results from the melting experiments. *Subindices* are: Mg number for Bt and Crd, % of An in Pl, % of En-Fs in Opx and % of Alm-Prp-Grs in Grt. Mineral abbreviations according to Kretz (1983). *Numbers in brackets* are the approximate modal composition for each mineral

Run number	*P* (kbar)	*T* (°C)	Added H_2O	Duration (h)	% Melt	Assemblages	Relic phases
A79710: Bt-Ms gneiss (Ollo de Sapo, coarse-grained facies)							
AC 4	3	900	0	79	25–30	Pl_{31}(8), Crd_{55} (14), $Opx_{40\text{-}60}$ (< 2), Al-silicate (2), Kfs (6)	Qtz, Pl, Bt, Kfs
AC 36		800	0	263	5–10	Bt_{54} (8), Crd_{48} (11), Pl_{23} (< 5), Al-silicate (6), Kfs (4)	Qtz, Pl, Bt, Kfs
AC 12		800	2	198	22–24	Crd_{46} (6), Bt_{43} (< 2), Pl_{20} (5), Kfs (< 5)	Qtz, Pl, Bt, Kfs
AC 1	6	900	0	181	14–16	$Grt_{69\text{-}23\text{-}4}$ (< 2), Bt_{51}(7), Crd_{65} (6), Spl (4), Al-silicate (4), Kfs (6)	Qtz, Pl, Bt, Kfs
AC 35		800	0	404	< 5	Bt_{44} (7), Al-silicate (< 5), Kfs (< 5)	Qtz, Pl, Bt, Kfs
AC 10		800	2	354	20	Bt_{48} (8), Pl_{23} (< 5), Kfs (10)	Qtz, Pl, Bt, Kfs
AC 2	10	900	0	160	10–12	$Grt_{70\text{-}18\text{-}6}$ (< 5), Bt_{46} (10), Pl_{22} (10), Al-silicate (8), Kfs (4)	Qtz, Pl, Bt, Kfs
AC 11		800	2	206	10–15	Bt_{45} (10), Pl_{20} (5)	Qtz, Pl, Bt, Kfs.
AC 24		800	0	261	< 5	Bt_{43} (6), Al-silicate (< 5), Kfs (8)	Qtz, Pl, Bt, Kfs
AC 3	15	900	0	108	< 8	$Grt_{63\text{-}26\text{-}11}$ (8), Bt_{62} (5), Ky (4), Kfs (12)	Qtz, Pl, Bt, Kfs
AC 9		800	2	208	10–12	$Grt_{62\text{-}14\text{-}18}$ (< 2), Bt_{44} (8), Pl_{21} (< 5) , Kfs (< 2)	Qtz, Pl, Bt, Kfs.
AC 25		800	0	121	Not found	$Grt_{67\text{-}13\text{-}16}$ (< 5), Bt_{40} (4)	Qtz, Pl, Bt, Kfs, Ms
A7972: Crd-Sil gneiss (Bercimuelle)							
AC 8	3	900	0	208	20–22	Crd_{50} (8), $Opx_{40\text{-}59}$ (2), Kfs (6)	Qtz, Pl, Bt, Kfs
AC 21		800	0	122	< 5	Crd_{49} (6), Bt_{50} (< 5), Pl_{20} (10), Kfs (8)	Qtz, Pl, Bt,Crd, Kfs
AC 36		800	0	263	25–30	Bt_{47} (6), Pl_{26} (8), Kfs (9)	Qtz, Bt, Pl, Kfs, Crd
AC 5	6	900	0	102	12–15	$Grt_{50\text{-}49\text{-}1}$ (< 5), Crd_{50} (10), $Opx_{42\text{-}57}$ (< 5), Spl (< 2), Kfs (8)	Qtz, Pl, Bt,Crd, Kfs
AC 35		800	0	404	< 5	Bt_{42}(7), Crd_{53} (< 5), Pl_{10} (< 5), Al-silicate (< 4), Kfs (< 5)	Qtz, Pl, Bt,Crd, Kfs
AC 7	10	900	0	102	< 5	$Grt_{61\text{-}33\text{-}4}$ (5), Bt_{44} (4), Al-silicate (6), Kfs (3)	Qtz, Pl, Bt, Kfs
AC 6	15	900	0	102	< 5	$Grt_{67\text{-}23\text{-}8}$ (8), Bt_{53} (5), St (4), Kfs (4)	Qtz, Pl, Bt, Kfs
A79711: Bt-Ms gneiss (Ollo de Sapo, fine-grained facies)							
AC 4	3	900	0	79	40–45	Crd_{64} (10), $Opx_{47\text{-}52}$ (5), Al-silicate (< 5), Spl (5),Pl_{22} (6), Kfs (8)	Qtz, Pl, Bt, Kfs
AC 1	6	900	0	181	40	$Grt_{59\text{-}32\text{-}3}$ (5), Bt_{54}(< 5), $Opx_{50\text{-}49}$ (< 10), Spl (< 5)	Qtz, Pl, Bt, Kfs
AC 2	10	900	0	160	12	$Grt_{66\text{-}20\text{-}6}$(< 5), Bt_{53} (8), Al-silicate (5), Kfs (< 5)	Qtz, Pl, Bt, Kfs
AC 3	15	900	0	108	8–10	$Grt_{58\text{-}34\text{-}7}$ (8), Bt_{72} (7), Ky (5), Pl_{16} (< 5), Kfs (10)	Qtz, Pl, Bt, Kfs
A7971: Granodiorite gneiss (La Almohalla gneiss)							
AC 8	3	900	0	208	< 10	$Opx_{30\text{-}69}$ (< 5), Pl_{40}(< 5), Kfs (< 5)	Qtz, Pl, Bt, Kfs
AC 5	6	900	0	102	< 5	$Grt_{74\text{-}16\text{-}7}$ (7), $Opx_{34\text{-}65}$ (< 2), Pl_{39} (< 2), Kfs (< 5)	Qtz, Pl, Bt, Kfs
AC 7	10	900	0	102	< 2	$Grt_{67\text{-}15\text{-}15}$ (8) , Bt_{37} (< 2), Kfs (< 5)	Qtz, Pl, Bt, Kfs
AC 6	15	900	0	102	< 2	$Grt_{64\text{-}14\text{-}21}$ (10), Bt_{55} (< 5), Kfs (6)	Qtz, Pl, Bt, Kfs
IT-521: Metagreywacke (Lower Cambrian/Upper Precambrian complex)							
AC21	3	800	0	122	< 2	Bt_{34} (5), Crd_{53} (10)	Qtz, Pl, Bt,Crd
AC 35	6	800	0	404	< 2	Bt_{31} (13), Crd_{45} (10)	Qtz, Pl, Bt,Crd
AC 24	10	800	0	261	Not found	Bt_{40} (< 5)	Qtz, Pl, Bt,Crd
AC 25	15	800	0	121	< 5	$Grt_{77\text{-}18\text{-}3}$ (5), Bt_{42} (10), Ky (< 5), St (< 5)	Qtz, Pl, Bt,Crd

Biotite

Biotite is present in runs at 6, 10 and 15 kbar, but not at 3 kbar. Biotite is absent from runs with high melt proportion, in which some Bt components are dissolved in the melt. Typically, neoformed Bt crystals are very small (2–5 μm) euhedral tablets. They appear included in glass, or at the boundaries between relict grains in the melt-absent runs. Their Mg# are fairly constant (0.55–0.62), but they display a continuous increase in Al content with *P* (see Patiño Douce et al. 1993). There is also a slight increase in the Mg# with *P* related to the appearance of almandine-rich garnet. Figures 7b, d and f show the typical aspect of neoformed biotites.

Cordierite

This is present in runs at 3 and 6 kbar at 800 and 900 °C and in experiments with both Bt-Ms-gneiss (Ollo de Sapo) and Crd-gneiss (Bercimuelle) starting materials. It occurs as euhedral, unzoned crystals (included in glass) and with inclusions of spinel in the 900 °C runs (Fig. 7a). In runs at 6 kbar, cordierite coexists with garnet. Pressure calculated using the compositions of Crd-Grt pairs applying the TWQ software (Berman 1991) are within error of the nominal experimental pressures. The Mg# of Crd increases with *P* from 0.55 at 3 kbar to 0.64 at 6 kbar. There is also an increase of the channel cations (Na,K) and water with *P*. The increase in H_2O content is inferred from analytical totals that are around 96% at 6 kbar and around 99% at 3 kbar.

Garnet

Garnet occurs as large (up to 100 μm), euhedral, poikilitic crystals in runs at 6, 10 and 15 kbar. It is more abundant in experiments on the Crd-gneiss than in those on the Bt-Ms-gneiss. Garnet always appears associated to relic biotite (Fig. 7c,d) and surrounded by glass, demonstrating that it is a peritectic phase, formed by the incongruent melting reaction of biotite. The average composition of garnet from the Ollo de Sapo and Bercimuelle gneisses is Alm_{86} Pyr_{24} $Gross_4$ $Spes_4$. The only noticeable variation is an increase of the Gross content with *P*, from 3 mol% at 6 kbar to 11 mol% at 15 kbar. There is a slight increase in Alm with *P* in runs on the Crd-gneiss (Bercimuelle). This variation mirrors the increase in Mg# of biotite.

Al silicate

This appears in all runs at 900 °C on the Bt-Ms-gneiss, but only at 6 and 10 kbar and 900 °C in experiments with the Crd-gneiss (Bercimuelle). Both starting materials have similar alumina saturation indices. In these runs neoformed mullite is associated with relic Ms and melt (Fig. 7e, f).

Al-rich spinel

This is only present in runs at 900 °C and at 6 and 10 kbar. It occurs as very small (1–2 μm), euhedral crystals that are difficult to analyse. Spinel is associated with Crd and melt at 6 kbar, and with Al silicate and melt at 10 kbar. It is more abundant in experiments on the Bt-Ms-gneiss.

K-feldspar

This appears in all melt-bearing run products, forming euhedral crystals that are either isolated in the melt (Fig. 7b, d, f), or surround relic plagioclase crystals (Fig. 7c). They are rich in orthoclase (>95 mol% Or). The euhedral habit and the association with melt pools and Bt relics indicate that Kfs is a phase associated to the melt producing reactions, from the breakdown of micas. In runs with a high melt proportion Kfs is less abundant compared with low melt fraction runs. This shows that Kfs is a product of the incongruent melting reaction, but that it then switches sides and becomes a reactant (see also Patiño Douce and Harris 1998). K-feldspar thus persists over a relatively narrow temperature interval above the dehydration-melting solidus (Patiño Douce and Johnston 1991; Patiño Douce and Beard 1995).

Plagioclase

Plagioclase is a phase that is generally consumed in the experimental runs. It only appears as a neoformed phase in low *P*, high *T* experiments. The composition of plagioclase in the starting materials is very variable, as they are volcanoclastic materials (5–20 mol% An). The same variation is found in the experimental runs suggesting that Pl does not re-equilibrate its composition during melting reactions.

Orthopyroxene

Orthopyroxene appears as skeletal, acicular crystals in high *T* runs (900 °C) at 3 and 6 kbar on the Crd-gneisses, and at 3 kbar only in Bt-Ms-gneiss runs. It is very scarce and appears only associated to relic Bt as a peritectic product of the melting reaction. Orthopyroxene composition is constant in different run products, about $En_{40}Fs_{60}$.

Quartz

Quartz is always a reactant phase. It appears as rounded grains included in glass. The proportion of Qtz is inversely correlated with the melt percentage, suggesting that this phase appears as relic because it is an excess phase, and not because of kinetic problems.

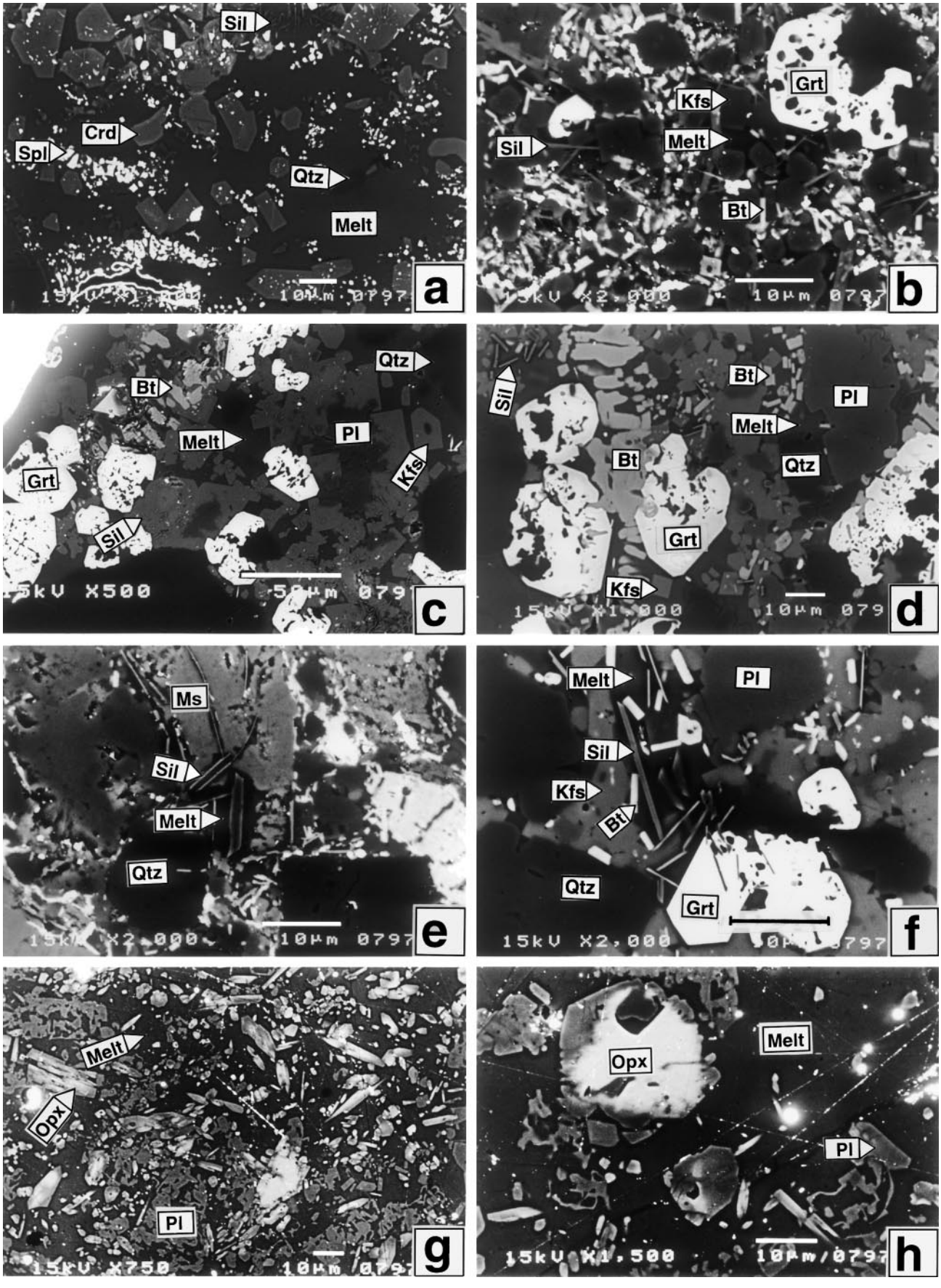
Sil
Crd
Spl
Qtz
Melt
a
Grt
Kfs
Sil
Melt
Bt
b
Qtz
Bt
Melt
Pl
Grt
Kfs
Sil
c
Sil
Bt
Pl
Melt
Bt
Qtz
Grt
Kfs
d
Ms
Sil
Melt
Qtz
e
Melt
Pl
Sil
Kfs
Bt
Qtz
Grt
15kV X2,000
f
Melt
Opx
Pl
g
Melt
Opx
Pl
15kV X1,500
h

◄

Fig. 7a–h Representative textures of experimental products. The photographs correspond to backscattered electron images (Z-contrast). Mineral labels according to the abbreviations of the IMA (Kretz 1983). The photographs correspond to the following runs (see Tables 4 and 5): **a** run AC4 sample A79710; **b, c** and **d** run AC3 sample A79710; **e** run AC2 sample A79711; **f** run AC7 sample A7972; **g** and **h** run AC19a. Note the difference in the melt content between a low-*P* run (**a**) and a high-*P* run (**b**). Textures in **c, d** and **e** evidence the production of melt associated to the breakdown of Bt and/or Ms. Note the homogeneous composition of Crd in **a** and the high melt fraction obtained in the assimilation experiments

Melt compositions

The compositions of melts formed in the experimental runs are given in Table 5. Melt compositions vary little with *P* or *T*. They match the compositions of peraluminous leucogranites with very low Fe + Mg content (< 2 wt%) and high alumina saturation index. They plot in the field of leucogranites of the A-B multicationic diagram (Fig. 8). The Mg# is difficult to determine by EDS analyses (specially for the lighter element Mg), as the concentrations of Fe and Mg are very low and close to the detection limit. However, it appears that Mg# of melts is generally higher in high *P* experiments that contain Grt than in low *P* experiments, that contain Crd. In other words, melts formed at high *P* are depleted in iron compared to melts formed at low *P*. Figure 9 shows variations in melt composition and melt fraction with *P*, at a constant *T* of 900 °C. The Na/K ratio increases with *P*, because Na_2O content increases with P. This trend is correlated with breakdown of plagioclase with increasing *P* (see also Patiño Douce 1995; Patiño Douce and Beard 1996). Note the low productivity of melt at high pressure, compared to the high melt proportions obtained in the low pressure experiments. The gneissic rock (Ollo de Sapo gneiss) is richer in Ms and is also the most fertile of the source materials studied. Pressure also affects the Al saturation index of the melts, albeit only slightly.

Assimilation experiments

We have also carried out assimilation experiments similar to those performed by Patiño Douce (1995) using a gabbro and two pelitic gneisses as the crustal end-members. Experimental conditions and phase assemblages in the run products are given in Table 6, and melt compositions are given in Table 7. Finely crushed and intimately mixed rock powders were used in all cases, with no added water. Because we used rock powders rather than glass there are some relic phases in the solid residue. The modal amount of these relic phases is always less than 10 vol.%, so they are likely to have minor effect on melt compositions. The modal percentages shown in Table 6 for neoformed phases and glass have been recast to 100%, disregarding the relic phases. Textural and chemical features of neoformed phases are as follows.

Orthopyroxene (20–30 vol.%)

This appears as a neoformed phase in all the assimilation experiments. It forms euhedral, occasionally dendritic crystals ranging in size from 1 μm to 50 μm. Most crystals are on the order of 10 μm (Fig. 7g,h). A slight zoning is observed only in larger crystals that contain a relic core, but the composition is nearly homogeneous in the smaller, completely neoformed crystals. The composition of Opx is very homogeneous and rich in En, which ranges from 81 to 88 mol%. The Al content is correlated with *P*, being slightly higher in the runs at 10 kbar (Al_2O_3 = 4.75 wt%) than in the runs at 4 kbar (Al_2O_3 = 2.35 wt%).

Plagioclase (15–30 vol.%)

This phase also appears in all the assimilation experiments. It forms dendritic (skeletal) crystals with a very uniform grain size averaging 10 μm (Fig. 7g, h). Larger crystals of up to 50 μm are present in some runs. The composition is very homogeneous (50–66% mol An) both within each run and comparing different runs. However, plagioclase is slightly more calcic in experiments at low pressure (4 kbar).

Melt compositions

Table 7 shows the average glass (quenched melt) compositions measured in the assimilation experiments. All the melts have the compositions of peraluminous granodiorites with $SiO_2 > 68$ wt%, CaO > 2 wt%, and positive values for the alumina saturation index ($A > 9$). It is important to note the low content in Fe + Mg + Ti ($B < 75$).

Attainment of equilibrium

The approach to equilibrium in melting and assimilation experiments on starting materials similar to those used here, and at comparable *P-T* conditions, was discussed in previous contributions. In particular, Patiño Douce and Beard (1995) used mineral compositions and reversals of phase assemblages (obtained by means of crystallisation experiments) to show that dehydration-melting experiments at temperatures of 900 °C approach equilibrium reasonably well. Patiño Douce (1995) showed that the same is true in assimilation experiments at 1000 °C, also on the basis of mineral compositions

Table 5 Melt compositions obtained in the melting experiments. $A = 1000 * [Al - (Na + K + 2\,Ca)]$, $B = 1000* (Fe + Mg + Ti)$. [(*n*) number of analyses]. SD: SiO_2 = (0.2–1.5); TiO_2 = (0.1–0.2); Al_2O_3 = (0.04–0.6); FeO = (0.1–0.2); MnO = (0.1–0.2); MgO = (0.03–0.45); CaO = (0.1–1.8); Na_2O = (0.04–0.33); K_2O = (0.1–0.6)

P (kbar)	*T* (°C)	Run no.	Added H_2O	(*n*)	SiO_2	TiO_2	Al_2O_3	FeO	MnO	MgO	CaO	Na_2O	K_2O	Total	100 - Total	A	B	Na/K
A79710: Bt-Ms gneiss (Ollo de Sapo. coarse-grained facies)																		
3	900	AC 4	0	4	76.3	0.35	13.6	1.00	0.00	0.12	0.34	2.91	5.42	100	4.86	45	21	0.82
	800	AC 36	0	3	77.3	0.20	14.2	0.90	0.07	0.00	0.54	3.02	3.78	100	6.17	81	15	1.21
	800	AC 12	2	10	76.9	0.18	14.3	1.11	0.07	0.10	0.53	3.20	3.61	100	6.96	82	20	1.35
6	900	AC 1	0	5	74.1	0.17	15.2	1.61	0.02	0.12	0.52	3.02	5.29	100	10.5	69	28	0.87
	800	AC 35	0	5	77.0	0.06	14.4	1.04	0.05	0.04	0.51	3.26	3.62	100	6.92	82	16	1.37
	800	AC 10	2	9	77.1	0.19	13.7	1.60	0.05	0.07	0.35	3.82	3.17	100	9.79	65	26	1.83
10	900	AC 2	0	5	74.1	0.17	15.9	1.41	0.07	0.22	0.70	3.49	3.93	100	9.24	90	27	1.35
	800	AC 11	2	12	75.2	0.07	16.1	1.25	0.10	0.10	0.70	3.80	2.74	100	9.22	110	21	2.11
	800	AC 24	0	3	70.6	0.29	16.5	2.08	0.08	0.59	0.66	4.21	5.00	100	6.10	59	47	1.28
15	900	AC 3	0	4	74.6	0.22	16.1	0.80	0.08	0.17	0.67	3.54	3.81	100	6.16	97	18	1.41
	800	AC 9	2	5	75.6	0.11	16.1	0.90	0.05	0.08	0.69	4.00	2.50	100	8.45	109	16	2.43
A7972: Crd-Sil gneiss (Bercimuelle)																		
3	900	AC 8	0	4	76.1	0.23	13.8	1.88	0.06	0.05	0.34	3.23	4.25	100	4.13	65	30	1.16
	800	AC 21	0	6	76.7	0.10	14.7	1.00	0.04	0.00	0.54	3.94	3.01	100	1.88	78	15	1.99
	800	AC 36	0	6	77.7	0.02	13.9	0.89	0.08	0.01	0.19	3.32	3.85	100	7.37	78	13	1.31
6	900	AC 5	0	5	75.2	0.31	14.7	1.48	0.10	0.20	0.46	3.41	4.12	100	4.08	75	29	1.26
	800	AC 35	0	5	73.1	0.02	16.9	1.17	0.09	0.12	0.93	3.71	3.94	100	6.91	95	20	1.43
10	900	AC 7	0	4	74.4	0.21	15.6	1.13	0.08	0.16	0.43	4.04	3.98	100	8.35	77	22	1.54
15	900	AC 6	0	5	74.1	0.13	16.3	0.84	0.03	0.15	0.52	4.25	3.76	100	6.47	84	17	1.72
A79711: Bt-Ms gneiss (Ollo de Sapo. fine-grained facies)																		
3	900	AC 4	0	10	75.8	0.28	13.9	1.01	0.06	0.16	0.29	2.90	5.56	100	4.90	51	22	0.79
6	900	AC 1	0	11	72.8	0.28	15.2	1.87	0.08	0.38	0.50	3.40	5.43	100	7.60	56	39	0.95
10	900	AC 2	0	9	73.2	0.16	15.5	1.21	0.00	0.16	0.58	3.94	5.30	100	8.88	43	23	1.13
15	900	AC 3	0	10	72.8	0.27	15.8	0.71	0.04	0.07	0.56	4.66	5.17	100	9.95	29	15	1.37
A7971: Granodiorite gneiss (La Almohalla gneiss)																		
3	900	AC 8	0	12	75.5	0.31	13.7	1.73	0.11	0.13	0.85	2.86	4.82	100	4.73	44	31	0.90
6	900	AC 5	0	10	74.1	0.33	14.3	1.97	0.17	0.26	0.76	3.41	4.78	100	8.23	41	38	1.08
10	900	AC 7	0	10	73.6	0.33	14.8	1.26	0.03	0.13	0.93	4.20	4.73	100	8.28	21	25	1.35
15	900	AC 6	0	10	72.7	0.47	15.9	1.32	0.09	0.19	0.91	4.55	3.87	100	9.67	50	29	1.79
IT-521: Metagreywacke (Lower Cambrian/Upper Precambrian complex)																		
6	800	AC 35	0	5	73.8	0.04	16.8	0.82	0.03	0.00	0.17	5.39	3.02	100	8.05	85	12	2.72

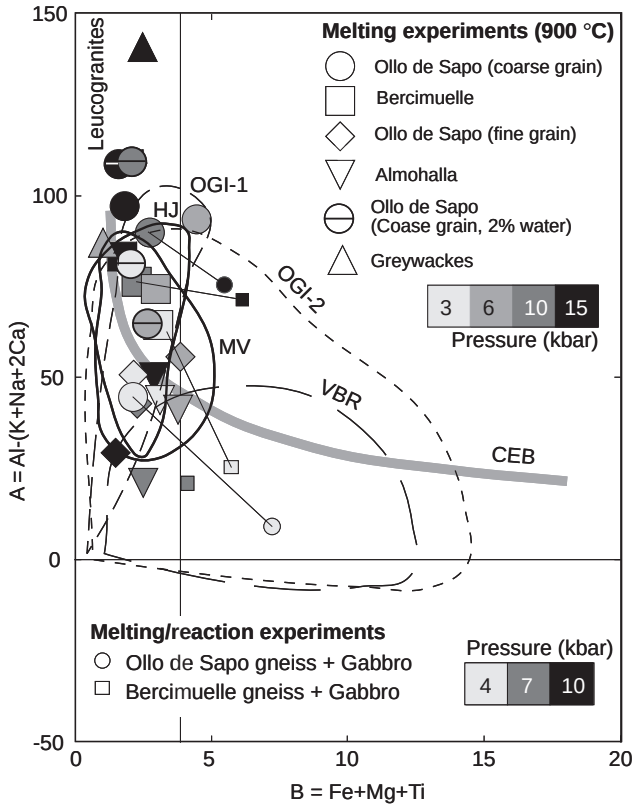

Fig. 8 A-B multicationic diagram (Debon and Le Fort 1983) showing the position of melts obtained in the melting and assimilation experiments. Melts tend to be richer in Al (A parameter) with P. All the melts developed from pelitic rocks have the composition of peraluminous leucogranites. Hybrid melts obtained in the gabbro-pelite assimilation experiments are also peraluminous and slightly richer in the B parameter. *Dashed lines* show the shift in the B parameter of melts produced from the same starting composition from a pure melting experiment towards the corresponding assimilation experiment. [*Labeled fields* are: *HJ* experimental melts of Holtz and Johannes (1991); *MV* experimental melts of Montel and Vielzeuf (1997); *CEB* trend of the Central Extremadura batholith (see Fig. 2); *OG-1* and *OG-2* fields of leucogranites and Bt-granites, respectively, from Galicia (Ortega and Gil Ibarguchi 1991); VBR Gredos (Spanish Central System) granites (Villaseca et al. 1998)]

and crystallisation experiments. In addition to these previous results, the following features of the experimental run products discussed here are good indicators that they, too, approached equilibrium reasonably well:

1. Neoformed minerals are always euhedral and notably unzoned. Although poikilitic crystals are common (e.g. garnet), skeletal crystals (which could denote metastable crystallisation) are almost completely absent, with the exception of Pl in the assimilation experiments.

2. Melt compositions are very uniform throughout the experimental charges.

3. Mineral compositions vary regularly and consistently with pressure and/or temperature. For example: garnet becomes enriched in Ca, and plagioclase depleted in Ca, with increasing pressure; cordierite generally becomes enriched in alkalis with decreasing pressure; and the octahedral Al content of biotite coexisting with garnet, sillimanite and quartz generally increases with increasing pressure and with decreasing temperature (see Patiño Douce et al. 1993). Biotite in experiments at 15 kbar tends to depart from this regular behaviour, probably because melting in these experiments is only incipient (see Table 4), and the residual biotite has not re-equilibrated as completely as in lower pressure experiments. These observation suggest that equilibrium is approached locally in the charges, but the presence in the experimental products of zoned phases (notably plagioclase) and of crystals of the same phase with different compositions (e.g. relic and neoformed biotite) shows that equilibrium is generally not attained throughout the entire volume of the charges. This problem was discussed in detail by Patiño Douce and Harris (1998), who concluded that, even if equilibrium is attained only locally, dehydration-melting experiments nevertheless provide reliable information on solidus temperatures, melt compositions, and melting reaction stoichiometries. Experimentally determined melt fractions, in contrast, can have larger uncertainties (see Patiño Douce and Harris 1998).

Discussion

The origin of peraluminous leucogranites

Dehydration-melting experiments carried out on natural crustal starting materials (greywackes**:** Conrad et al. 1988; Vielzeuf and Montel 1994; Patiño Douce and Beard 1995, 1996; Patiño Douce 1996; Patiño Douce and McCarthy in press; pelites and pelitic gneisses**:** Vielzeuf and Holloway 1988; Patiño Douce and Johnston 1991; Holtz and Johannes 1991; Gardien et al. 1995; Patiño Douce and Harris 1998) have demonstrated that melt compositions are leucogranitic for conditions of P and water contents comparable to those of potential sources in the continental crust. The melting experiments presented in this study are in agreement with these previous findings. The compositions of melts (Table 5) from experiments at different pressures and temperatures, and carried out on different starting materials, are all peraluminous and all have very low contents of Fe and Mg. These melts match the composition of most migmatitic leucosomes, anatectic autochthonous granites and allochthonous, two-mica granites, as shown in the multicationic diagram of Figs. 8 and 2. The results of the melting experiments presented in this paper have the following implications on the origin of the Iberian peraluminous leucogranites:

1. The La Almohalla granodiorite gneiss is not a suitable source rock for leucogranite magmas, because it starts melting at high temperature (approximately 900 °C), and even at this temperature it produces less than 5 vol.% melt. The explanation of this behaviour rests on its igneous bulk composition, which is poor in mica, and therefore relatively dry, compared to meta-

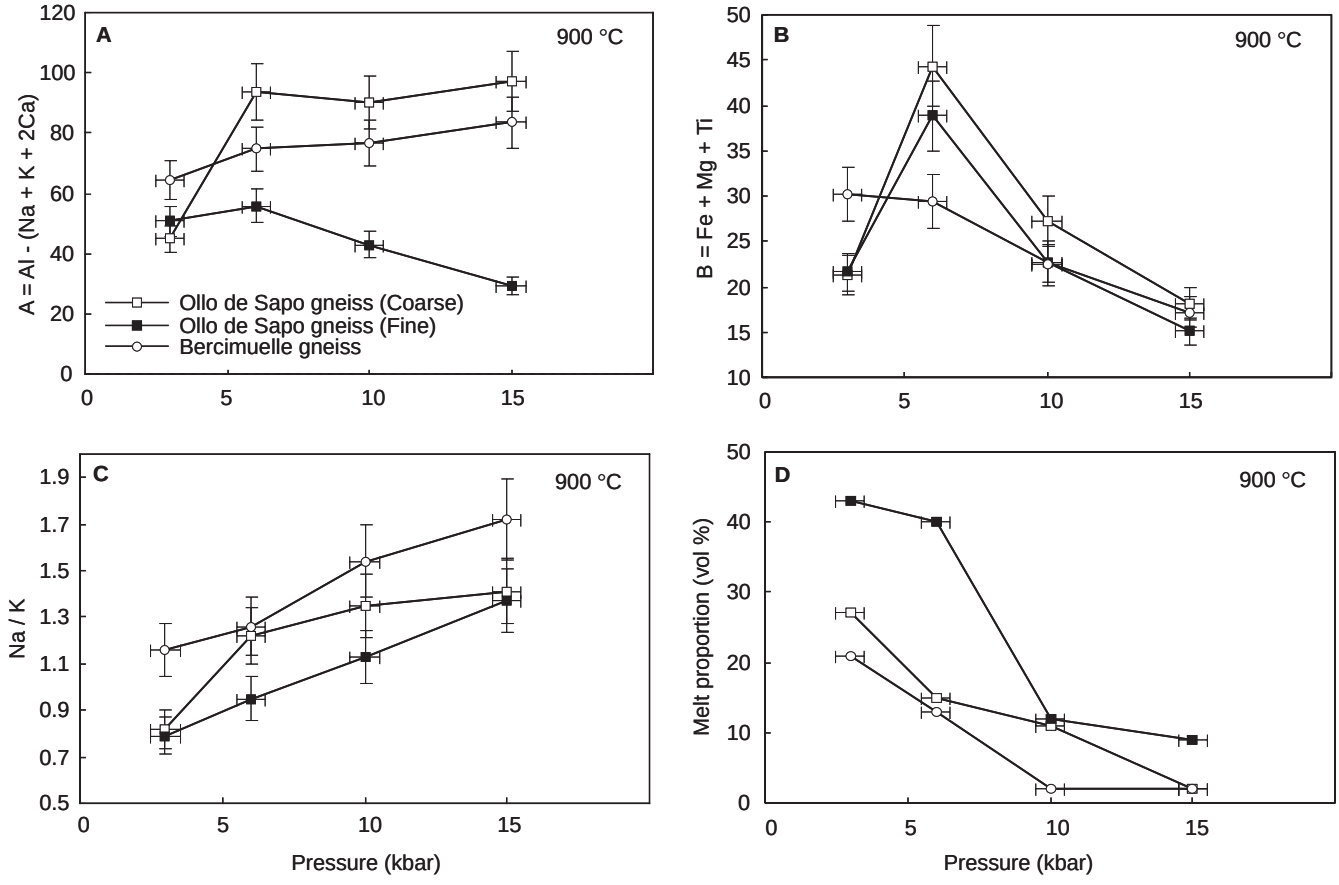

Fig. 9A–D Variations in melt compositions (**A, B** and **C**) and melt proportion (**D**) with pressure at 900 °C for the pelitic gneisses used in the melting experiments. The Na/K ratio increases with *P*. The B parameter ranges within a narrow range. The low values of MgO near to the detection limit of the EDS analyser are the main reason for the observed variation. Note the low productivity of melt at high pressure compared with the high proportions obtained in the low pressure experiments

Table 6 Experimental conditions and summarised results from the assimilation experiments. *Subindices* are: mol% of En, Fs and Wo in Px and mol% of An in Pl. *In brackets* are : approximated modal compositions

Run no.	*T* (°C)	*P* (kbar)	Duration (h)	Vol% melt	Assemblage
50% Gabbro (Puente del Congosto complex) + 50% Crd-Sill gneiss (Bercimuelle)					
AC41a	1000	4	172	60	$Opx_{85\text{-}13\text{-}2}$ (28), Pl_{65} (12)
AC19a	1000	10	223	58	$Opx_{82\text{-}16\text{-}2}$ (23), Pl_{51} (19), Rt
50% Gabbro (Puente del congosto complex) + 50% Bt-Ms gneiss (Ollo de Sapo, coarse-grained facies)					
AC41b	1000	4	172	61	$Opx_{88\text{-}10\text{-}2}$ (19), Pl_{66} (19), Rt
AC42a	1000	7	171	52	$Opx_{81\text{-}17\text{-}2}$ (24), Pl_{57} (24), Rt
AC19b	1000	10	223	59	$Opx_{83\text{-}15\text{-}2}$ (21), Pl_{58} (20)

Table 7 Melt compositions obtained in the assimilation experiments. [(*n*) number of analyses] $A = 1000 * [Al - (Na + K + 2 Ca)]$, $B = 1000*(Fe + Mg + Ti)$, SD: SiO_2 = (0.2–1.5), TiO_2 = (0.1–0.2), Al_2O_3 = (0.04–0.6), FeO = (0.1–0.2), MnO = (0.1–0.2), MgO = (0.03–0.45), CaO = (0.1–1.8), Na_2O = (0.04–0.33), K_2O = (0.1–0.6)

T (°C)	*P* (kbar)	Run no.	Added H_2O	(*n*)	SiO_2	TiO_2	Al_2O_3	FeO	MnO	MgO	CaO	Na_2O	K_2O	Total	100-Total	A	B	Na/K
50% Gabbro (Puente del Congosto complex) + 50% Crd-Sil gneiss (Bercimuelle)																		
1000	4	AC 41a	0	5	68,26	0,74	16,96	1,30	0,00	1,81	4,04	3,23	3,67	100,00	5,62	9	72	1,34
	10	AC 19a	0	10	71,02	0,84	16,92	1,15	0,00	1,15	3,06	2,11	3,80	100,00	7,63	75	54	0,84
50% Gabbro (Puente del Congosto complex) + 50% Bt-Ms gneiss (Ollo de Sapo, coarse grained facies)																		
1000	4	AC 41b	0	4	69,49	0,92	16,70	0,81	0,00	1,37	2,97	3,17	4,56	100,00	6,68	24	57	1,06
	7	AC 42a	0	7	72,18	0,56	15,30	1,16	0,00	0,71	2,26	2,99	4,84	100,00	7,87	21	41	0,94
	10	AC 19b	0	14	70,44	0,83	17,07	1,39	0,03	1,26	3,49	2,18	3,28	100,00	7	72	61	1,01

sedimentary rocks (Patiño Douce and Johnston 1991; Patiño Douce 1997). The melts obtained from this protolith are nevertheless peraluminous leucogranites, similar to those obtained from greywackes and gneisses. Leucogranite melts can thus be produced by high temperature melting of granodiorite protoliths, but the low melt productivity of these protoliths would require the involvement of unreasonably large volumes of granodiorite to generate plutons of leucogranite.

2. Greywackes and gneisses (Ollo de Sapo and Bercimuelle) give similar melts at similar conditions of P and T. Only small differences in melt compositions and melt proportions are found. That is, there is no single identifiable source for the generation of peraluminous leucogranites in the Iberian massif.

3. Peraluminous leucogranites may represent pure melts extracted from a pelitic crustal source, under fluid-absent conditions and leaving a solid residue rich in garnet or cordierite, depending on the pressure of partial melting (Table 4). The positive slope of the dry solidus determined for the Ollo de Sapo gneiss (Castro et al. in litt) implies that melting is favoured at low P and during decompression, in agreement with the observed field relationships that indicate syn-extensional anatexis. Only the autochthonous leucogranites may have some restitic material that was not separated from the melt. Similar results were obtained by Holtz and Johannes (1991) for peraluminous granites of northern Portugal.

4. The scarcity of restitic material in these leucogranites implies that nearly all Fe and Mg were dissolved in the melt producing cordierite in some cases and biotite ± muscovite in other cases depending on the water content of the melts. Consequently, restite unmixing is not an important mechanism in producing compositional variations in these granites.

The origin of peraluminous Bt-granodiorites and Crd-monzogranites

The major element compositions of the peraluminous Bt-granodiorites and Crd-monzogranites do not match those of the melts generated from the range of crustal rocks present in the studied area (CIZ) (Fig. 8). This discrepancy, together with the isotopic compositions of these granitoids, argues for the presence of juvenile mantle material in the granodiorites and monzogranites. As we discussed earlier, this must have been incorporated at the time of generation of the granitoid magmas by complete assimilation of crustal rocks by mafic magmas. This mechanism was originally proposed by Bowen (1922, 1928) as a reaction process acting in the direction of the reaction series, and producing large volumes of granitic liquids while at the same time transforming the basaltic magmas into noritic cumulates. It must be emphasised that this process is not one of simple assimilation nor one of magma mixing, in which the resulting magma has some intermediate composition between two end-members. Rather, and as clearly pointed out by Bowen (1922, 1928), it is a process in which solid rocks are dissolved into silicate melts, changing the composition of the melts and also precipitating solid assemblages that will generally differ from those being dissolved and from those that would crystallise from the silicate melt in the absence of assimilation. This process was addressed in a general way by Patiño Douce (1995), who studied experimentally reactions between a high-Al olivine tholeiite and different kinds of crustal rocks.

The presence of mantle-derived magmas associated to granodiorites in magma mixing zones (e.g. Puente del Congosto) argues in favour of basalt-crust reactions. The fact that these magmas are coeval with the granodiorites shows that mantle magmatism was synchronous with partial melting of crustal materials. However, the observed magma mingling zones represent late stages of magmatic activity, that must have been formed after the process of reaction and assimilation that gave rise to the granodiorite magmas themselves. This sequential interpretation is based on the fact that the felsic end-member found in the magma mixing zones is already hybrid granodiorite. Leucogranites (which represent the end-member crustal melts) are never found in mixing zones. Another argument in favour of this assimilation process is the common presence in the peraluminous granodiorites of the Iberian massif (Central System and Galicia) of gabbroic rock of clear cortlandtitic affinity. Noritic cortlandtites are characterised by the assemblage Opx Pl with interstitial and poikilitic phlogopite and amphibole. These rocks may represent the noritic residues left after the extraction of the hybrid granodiorite melts. Bowen (1922, p. 551) considered the rocks of Cortlandt as typical examples of the residual products formed by reaction of basaltic magmas with pelitic rocks.

The results of the assimilation experiments presented in this paper, using a gabbro and two kind of gneisses, are in good agreement with the results of Patiño Douce (1995). In summary, the experiments show the following: (1) the formation of a high proportion of melt (around 50 vol.%), regardless of pressure; (2) the production of a norite residue, composed of plagioclase and orthopyroxene; (3) the peraluminous nature of the melts, with alumina content increasing with pressure; (4) the granodioritic composition of the melts, with CaO > 2 wt%.

When compared with the natural rocks, however, the experimental melts are poorer in Mg + Fe than normal Bt-Crd-granodiorites. The experimental hybrid melts are K-rich leucogranodiorites that do not exceed a value of 60 for the B parameter (Fig. 8) in the multicationic A-B diagram of Debon and Le Fort (1983). Most granodiorites of the Iberian massif plot in a broad field that reaches values of up to B = 200, or greater.

The Mg + Fe content of the experimental melts resulting from complete assimilation is determined by the saturating mineral assemblage (Opx + Pl). This assemblages clearly restricts Mg contents in granodiorite

melts at 1000 °C to very low values. A possible explanation for the discrepancy between experiments and nature is to assume that natural granodiorites do not represent pure melts, but rather contain some entrained residual phases. Given the high-Mg content of Opx ($B = 800$), between 0% and 20% of opx is needed to account for the complete compositional variation in the B parameter of natural granodiorites. When the granodiorite melt is extracted from the melting-reaction (assimilation) region carrying part of the solid residue (Pl + Opx), changes in P and perhaps water activity may cause Opx to enter into a reaction relationship with the melt, to produce Crd + Bt in peraluminous melts, or Amp + Bt in metaaluminous granodiorite melts. Crystallisation of cordierite by reaction between orthopyroxene and melt can be modelled as follows (see also Patiño Douce 1992):

$$2\,MgSiO_3 + SiO_2 + 2\,[Al_2SiO_5]_{melt} + n\,[H_2O]_{melt} \leftrightarrow Mg_2Al_4Si_5O_{18} \cdot n\,H_2O$$

This reaction is displaced to the right by a decrease in pressure, and by increases in the chemical potentials of alumina and H_2O in the melt (Patiño Douce 1992). At least two of these variables shift in the direction of stabilising cordierite during segregation, ascent and crystallisation of the hybrid granodiorite melts: pressure decreases, and H_2O content of the melt increases by crystallisation of anhydrous phases (e.g. feldspars). Cordierite in the hybrid granodiorites and monzogranites may thus be, at least in part, the product of orthopyroxene-melt reactions. The presence of amphibole clots in granodiorites and associated enclaves, interpreted by Castro and Stephens (1992) as products of px-melt reaction, is another argument in favour of the presence of solid material (Opx) dragged by the melt in the course of extraction from the crustal assimilation region. Furthermore, some plagioclase may be incorporated in the granodiorite magma, accounting for the presence of relic An-rich cores in plagioclases in the granodiorites. This is one of the most characteristic textural features of these rocks (Castro and de la Rosa 1994; Castro et al. 1991). These experiments also show that simple binary mixing hypotheses will yield misleading results when trying to determine the relative proportions of mantle and crust by using the composition of the hybrid magma. This magma represents only part (perhaps 50% or so) of the products of a hybridisation reaction, in which a norite residue is also produced.

Granitoid magmatism and crustal growth

The isotopic and experimental approaches complement each other in providing a clear picture of the origin of the Hercynian granitoids of the Central Iberian zone of the Iberian massif. Isotopic compositions show that a sizeable input of juvenile mantle material must have taken place when the granitoid magmas were generated. Experiments show that assimilation of crustal rocks by basaltic magmas can account for such input, and that it leads to silica-rich magma compositions that closely resemble those of the isotopically hybrid peraluminous granodiorites. The experiments also show that a complementary suite of hybrid mafic noritic cumulate rocks must exist in the deep crust of the Iberian massif.

Processes of hybridisation and assimilation like the ones that we propose are a recurrent and fundamental aspect of crustal growth and crustal evolution, albeit with some degree of variability controlled by local differences in crustal thickness, thermal regimes, end-member compositions, and relative amounts of crustal and mantle components (e.g. Patiño Douce 1995).

The abundance of granitoid rocks in the Iberian peninsula that have a significant proportion of juvenile mantle material in their parentage indicates that the Hercynian orogenic cycle was an important episode of crustal growth. This crustal growth, however, did not take place by simple underplating or intraplating of basaltic material. Rather, the process entailed widespread interactions between juvenile mafic magmas and older crustal rocks. The products of such a process are hybrid silicic magmas and hybrid granulitic cumulates of broadly noritic composition. The former are now exposed at the surface as the extensive batholiths in the Central Iberian zone, composed of peraluminous granodiorites and monzogranites. The latter are known to constitute an important part of the lower continental crust, as evidenced by the European Geotraverse (e.g. Wedepohl 1995). This episode of Hercynian crustal growth may have been comparable in scale to Proterozoic episodes of crustal growth, such as the one that took place over the period 1.2 – 0.9 Ga (e.g. Taylor and McLennan 1985). In both cases crustal growth was coincident with major orogenic events, in agreement with the proposal of Stein and Hoffman (1994) that major increments in the volumes of the continents take place during orogenesis.

Acknowledgements This study has been supported by grants from the Spanish Science Commission (CICYT, project PB94-1085), the Andalousian government (Grant RNM120) and the University of Huelva. The acquisition of the experimental laboratory was founded by the European Commission (FEDER grants). A. Patiño-Douce supervised the installation of the experimental petrology laboratory in Spain during a sabbatical leave funded by the Spanish Science Commission (CICYT, Grant SAB95-0558). Emilio Ariño (Oviedo) assisted with XRF analyses. A. Castro also thanks Lola Pereira (Univ, Salamanca) for introducing him to the geology of the Peña Negra anatectic complex. François Holtz provided constructive criticism that considereably helped to improve the manuscript.

References

Allègre CJ, Ben Othman D (1980) Nd-Sr isotopic relationship in granitoid rocks and continental crust development: a chemical approach to orogenesis. Nature 286: 335–341

Beetsma JJ (1995) The Late Proterozoic/Paleozoic and Hercynian crustal evolution of the Iberian massif, N Portugal. PhD thesis, Vrije Univ

Berman RG (1991) Thermobarometry using multiequilibrium calculations: a new technique with petrologic applications. Can Mineral 29: 833–855

Bowen NL (1922) The behavior of inclusions in igneous magmas. J Geol 30: 513–570

Bowen NL (1928) The Evolution of the igneous rocks. Princeton Univ Press, Princeton

Capdevila R, Corretgé G, Floor P (1973) Les granitoides Varisques de la Meseta Ibérique. Bull Soc Géol Fr XV-3-4: 209–228

Casquet C, Fuster JM, González-Casado JM, Peinado M, Villaseca C (1988) Extensional tectonics and granite emplacement in the Spanish Central System: a discussion. In: Banda E, Mendes-Victor LA (eds) Proc 5th Workshop European Geotraverse (EGT) Project: The Iberian Peninsula, Eur Sci Foundation 65–76

Castro A (1986) Structural pattern and ascent model in the Central Extramadura batholith, Hercynian belt, Spain. J Struct Geol 8: 633–645

Castro A, de la Rosa JD (1994) Nomarski study of zoned plagioclase from granitoids of the Seville range batholith, SW Spain. Petrogenetic implications. Eur J Mineral 6: 647–656

Castro A, Fernández C (1998) Granite intrusion by externally induced growth and deformation (G-D) processes of the magma reservoir: the example of the Plasenzuela pluton, Spain. J Struct Geol 20: 1219–1228

Castro A, Stephens WE (1992) Amphibole-rich polycrystalline clots in calc-alkaline granitic rocks and their enclaves. Can Mineral 30: 1093–1112

Castro A, Moreno-Ventas I, de la Rosa JD (1991) H-type (hybrid) granitoids: a proposed revision of the granite-type classification and nomenclature. Earth-Sci Rev 31: 237–253

Collins WJ (1996) Lachlan Fold Belt granitoids: products of three component mixing. Trans R Soc Edinburgh Earth Sci 87: 171–181

Conrad WK, Nicholls IA, Wall VJ (1988) Water-saturated and -undersaturated melting of metaluminous and peraluminous crustal composition at 10 kbar: evidence for the origin of silicic magmas in the Taupo Volcanic Zone, New Zealand, and other occurrences. J Petrol 29: 765–803

Corretgé LG (1971) Estudio petrológico del batolito de Cabeza de Araya (Cáceres). PhD thesis, Univ Salamanca

Corretgé LG, Ugidos JM, Martínez FJ (1977) Les series granitiques du secteur Centre-Occidental Espagnol: la chaine varisque d'Europe moyenne et occidentale. Collon Int CNRS: Rennes 243: 453–461

Corretgé LG, Bea F, Suárez O (1985) Las características geoquímicas del batolito de Cabeza de Araya (Cáceres, España): implicaciones petrogenéticas. Trab Geol Univ Oviedo 15: 219–238

Debon F, Le Fort P (1983) A chemical-mineralogical classification of common plutonic rocks and associations. Trans R Soc Edinburgh Earth Sci 73: 135–149

De la Roche H (1978) La chimie des roches présentée et interpretée d'aprés la structure de leur facies mineral dans l'espace des variables chimiques: fonctions specifiques et diagrammes qui s'en deduisent aplication aux roches ignées. Chem Geol 21: 63–87

Doblas M (1991) Late Hercynian extensional and transcurrent tectonics in central Iberia. Tectonophysics 191: 325–334

Fernández C (1991) Estudio de los procesos de deformación en la zona de cizalla de Hiendelaencina (Sistema Central Español). PhD thesis, Ediciones Univ Complutense, Madrid

Fernández C, Castro A, de la Rosa JD, Moreno Ventas I (1997) Rheological aspects of magma transport inferred from rock structures. In: Bouchez JL, et al (eds) Granite: from segregation of melt to emplacement fabrics. Kluwer Academic Publishers, Dordrecht, pp 75–91

Fourcade S, Javoy M (1991) Sr-Nd-O isotopic features of mafic microgranular enclaves and host granitoids from the Pyrenees, France: evidence for their hybrid nature and inference on their origin. In: Didier J, Barbarin B (eds) Granites and their enclaves, 2nd edn. Elsevier, Amsterdam, pp 345–364

Galán G, Pin C, Duthou J (1996) Sr-Nd isotopic record of multistage interactions between mantle-derived magmas and crustal components in a collision context. The ultramafic-granitoid association from Vivero (Hercynian belt, NW Spain). Chem Geol 131: 467–91

Gardien V, Thompson AB, Grujic D, Ulmer P (1995) Experimental melting of biotite + plagioclase + quartz + -muscovite assemblages and implications for crustal melting. J Geophys Res 100: 15581–15591

Holden P, Halliday AN, Stephens WE (1987) Neodymium and strontium isotope content of microdiorite enclaves points to mantle input to granitoid production. Nature 330: 53–55

Holtz F, Johannes W (1991) Genesis of peraluminous granites. I. Experimental investigation of melt composition at 3 and 5 kbar and various H_2O activities. J Petrol 32: 909–934

Ibarrola E, Villaseca C, Vialette Y, Fuster JM, Navidad M, Peinado M, Casquet C (1987) Dating of Hercynian granites of the Sierra de Guadarrama (Spanish Central System). In: Bea F, Carnicero E, Gonzalo JC, López Plaza M, Rodríguez MD (eds) Geologia de los granitoides y rocas asociadas del Macizo Hesperico libro homenaje a L. C. Garcia de Figuerola. Rueda, Madrid, pp 377–384

Julivert M, Fontboté JM, Ribeiro A, Conde LN (1974) Memoria explicativa del Mapa Tectónico de la PenÌnsula Ibérica y Baleares. IGME, Madrid

Kagami H, Ulmer P, Hansmann W, Dietrich V, Steiger RH (1991) Nd-Sr isotopic and geochemical characteristics of the Southern Adamello (Northern Italy) intrusives: implications for crustal versus mantle origin. J Geophys Res 96: 14331–14346

Kretz R (1983) Symbols for rock-forming minerals. Am Mineral 68: 277–279

Lancelot JR, Allegret A, Iglesias M (1985) Outline of Upper Precambrian and Lower Paleozoic evolution of the Iberian Peninsula according to U-Pb dating of zircons. Earth Planet Sci Lett 74: 325–337

Montel JM, Vielzeuf D (1997) Partial melting of metagreywackes, II. Compositions of minerals and melts. Contrib Mineral Petrol 128: 176–196

Montero P, Bea F (1998) Accurate determination of Rb^{87}/Sr^{86} and Sm^{147}/Nd^{144} ratios by inductively coupled plasma mass spectrometry in isotope geoscience: an alternative to isotope dilution analysis. Anal Chim Acta 358: 227–233

Moreno-Ventas I, Rogers G, Castro A (1995) The role of hybridization in the genesis of Hercynian granitoids in the Gredos massif. inferences from Sm/Nd isotopes. Contrib Mineral Petrol 120: 137–149

Nägler TF, Schäfer HJ, Gebauer D (1995) Evolution of the western European continental crust: implications from Nd and Pb isotopes of Iberian sediments. Chem Geol 121: 345–357

Oen IS (1958) The geology, petrology and ore deposits of the Viseu region, Northern Portugal. Commun Serv Geol Port 41: 5–199

Oen IS (1970) Granite intrusion, folding and metamorphism in central northern Portugal. Bol Geol Mineral 81: 271–298

Ortega LA, Gil Ibarguchi JI (1990) The genesis of Late Hercynian granitoids from Galicia (Northwestern Spain): inferences from REE studies. J Geol 98: 189–211

Pankhurst RJ, Hole MJ, Brook M (1988) Isotope evidence for the origin of Andean granites. Trans R Soc Edinburgh Earth Sci 79: 123–133

Patiño Douce AE (1992) Calculated relationships between activity of alumina and phase assemblages of silica-saturated igneous rocks: petrogenetic implications of magmatic cordierite, garnet and aluminosilicate. J Volcanol Geothermal Res 52: 43–63

Patiño Douce AE (1995) Experimental generation of hybrid silicic melts by reaction of high-Al basalts with metamorphic rocks. J Geophys Res 100: 15623–15639

Patiño Douce AE (1996) Effects of pressure and H_2O content on the compositions of primary crustal melts. Trans R Soc Edinburgh Earth Sci 87: 11–21

Patiño Douce AE (1997) Generation of metaluminous A-type granites by low-pressure melting of calc-alkaline granitoids. Geology 25: 743–746

Patiño Douce AE, Beard JS (1994) H_2O loss from hydrous melts during fluid-absent piston-cylinder experiments. Am Mineral 79: 585–588

Patiño Douce AE, Beard JS (1995) Dehydration melting of biotite gneiss and quartz amphibolite from 3 to 15 kbar. J Petrol 36: 707–738

Patiño Douce AE, Beard JS (1996) Effects of P, $f(O_2)$ and Mg/Fe ratio on dehydration melting of model metagreywackes. J Petrol 37: 999–1024

Patiño Douce AE, Harris N (1998) Experimental constraints on Himalayan anatexis. J Petrol 39: 689–710

Patiño Douce AE, Johnston AD (1991) Phase equilibria and melt productivity in the pelitic system: implications for the origin of peraluminous granitoids and aluminous granulites. Contrib Mineral Petrol 107: 202–218

Patiño Douce AE, McCarthy TC (1998) Melting of continental rocks during continental collision and subduction. In: B Hacker, JG Liou (eds) When continents collide: geodynamics and geochemistry of ultra-high pressure rocks. Kluwer Academic Publishers, Dordrecht, pp 27–55

Patiño Douce AE, Johnston AD, Rice JM (1993) Octahedral excess mixing properties in biotite: a working model with applications to geobarometry and geothermometry. Am Mineral 78: 115–131

Pereira MD (1992) El complejo Anatéctico de la Peña Negra (Batolito de Avila): un estudio de la anatexia cortical en condiciones de baja presión. PhD thesis. Univ Salamanca

Pereira MD, Bea F (1994) Cordierite-producing reactions in the Peña Negra complex, Avila batholith, Central Spain: the key role of cordierite in low-pressure anatexis. Can Mineral 32: 763–780

Pin C (1991) Sr-Nd isotopic study of igneous and metasedimentary enclaves in some Hercynian granitoids from the Massif Central, France. In Didier J, Barbarin B (eds) Granites and their enclaves, 2nd edn. Elsevier, Amsterdam, pp 333–343

Pinarelli L, Rottura A (1995) Sr and Nd isotopic study and Rb-Sr geochronology of the Bejar granites, Iberian Massif, Spain. Eur J Mineral 7: 577–589

Roberts MP, Clemens JD (1993) Origin of high-potassium, calc-alkaline, I-type granitoids. Geology 21: 825–828

Rodríguez Alonso MD (1985) El complejo esquisto-grauváquico y el Paleozoico en el Centro-Oeste español. Acta Salmant 51, Ed Univ Salamanca, Salamanca

Schermerhorn LJG (1956) Igneous, metamorphic and ore geology of the Castro Daire-Sao Pedro do Sul-Satao region (Northern Portugal). Commun Serv Geol Port 27: 5–617

Serrano Pinto M (1983) Geochronology of Portuguese granitoids: a contribution. Stud Geol Salmant 18: 277–306

Serrano Pinto M, Casquet C, Ibarrola E, Corretgé LG, Portugal Ferreira M (1987) Sintese geocronologica dos granitoides Maciço Hesperico. In: Bea, et al (eds) Geología de los granitoides y rocas asociados del macizo Hespérico. Ed Rueda, Madrid, pp. 69–86

Skjerlie KP, Patiño Douce AE (1995) Anatexis of interlayered amphibolite and pelite at 10 kbar: effect of diffusion of major components on phase relations and melt fraction. Contrib Mineral Petrol 122: 62–78

Stein M, Hofmann AW (1994) Mantle plumes and episodic crustal growth. Nature 372: 63–68

Taylor SR, McLennan SM (1985) The continental crust: its composition and evolution. Blackwell Scientific Publications, Oxford

Turpin L, Cuney M, Friedrich M, Bouchez JL, Aubertin M (1990) Meta-igneous origin of Hercynian peraluminous granites in NW French Massif Central: implications for crustal history reconstructions. Contrib Mineral Petrol 104: 163–172

Ugidos JM, Valladares MI, Recio C, Rogers G, Fallick AE, Stephens WE (1997a) Provenance of Upper Precambrian–Lower Cambrian shales in the Central Iberian Zone, Spain: evidence from a chemical and isotopic study. Chem Geol 136: 55–70

Ugidos JM, Armenteros I, Barba P, Valladares MI, Colmenero JR (1997b) Geochemistry and petrology of recycled orogen-derived sediments: a case study from Upper Precambrian siliciclastic rocks of the Central Iberian Zone, Iberian Massif, Spain. Precambrian Res 84: 163–180

Vielzeuf D, Holloway JR (1988) Experimental determination of the fluid-absent melting relations in the pelitic system. Contrib Mineral Petrol 98: 257–276

Vielzeuf D, Montel JM (1994) Partial melting of Al-metagreywackes. 1. Fluid-absent experiments and phase relationships. Contrib Mineral Petrol 117: 375–393

Vigneresse JL, Bouchez JL (1997) Interaction between batches of granitic magma during pluton emplacement: the case of Cabeza de Araya (Spain). J Petrol 38: 1767–1776

Villaseca C, Barbero L, Rogers G (1998) Crustal origin of Hercynian peraluminous granitic batholiths of Central Spain: petrological, geochemical and isotopic (Sr, Nd) constraints. Lithos 43: 55–79

Wedepohl KH (1995) The composition of the continental crust. Geochim Cosmochim Acta 59: 1217–1232

Wildberg HGH, Bischoff L, Baumann A (1989) U-Pb ages of zircons from metaigneous and metasedimentary rocks of the Sierra de Guadarrama: implications for the Central Iberian crustal evolution. Contrib Mineral Petrol 103: 253–262